Single-nuclei RNA sequencing uncovers non-cell autonomous changes in cerebellar astrocytes and oligodendrocytes that may contribute to Spinocerebellar Ataxia Type 1 (SCA1) pathogenesis

Abbreviated title: Cell specific alterations in SCA1

Ella Borgenheimer[1#], Ying Zhang[1,2,3], Marija Cvetanovic[1,2*]

1. Department of Neuroscience, University of Minnesota
2. Institute for Translational Neuroscience, University of Minnesota 2101 6th Street SE, Minneapolis, MN 55455
3. Minnesota Supercomputing Institute, University of Minnesota

Current address: Baylor College of Medicine Graduate School of Biomedical Sciences

*Corresponding Author:

Marija Cvetanovic, Department of Neuroscience, University of Minnesota

2101 6th Street SE, Minneapolis, MN 55455

E-mail: mcvetano@umn.edu

Tel. 612-626-4918

Abstract (203 words)

Glial cells, including astrocytes and oligodendrocytes are important for normal brain function. In many neurodegenerative diseases glial cells undergo significant morphological, functional and gene expression changes termed reactive gliosis. The cause, identity and neuroprotective or neurotoxic nature of these changes remains incompletely understood. This knowledge in needed to develop a framework of how individual pathological changes in glial cells contribute to progressive dysfunction and selective neuronal vulnerability in neurodegenerative diseases. This is particularly relevant during the early disease stages that allow for the effective therapies and reversal or slowing of disease phenotypes. Spinocerebellar ataxia type 1 (SCA1) is a progressive neurodegenerative disease caused by an abnormal expansion of CAG repeats in the gene *Ataxin1* (*ATXN1*). While mutant ATXN1 is expressed broadly throughout the brain, SCA1 is characterized by severe degeneration of cerebellar Purkinje cells (PCs). Despite major advances in dissecting the effects of mutant ATXN1 on Purkinje cells, much less is understood how cerebellar astrocytes and oligodendrocytes respond to and contribute to Purkinje cell dysfunction in SCA1. To address this question we performed cerebellar single nuclei RNA sequencing (snRNA seq) of early disease stage *Pcp2-ATXN1[82Q]* mice, a transgenic SCA1 mouse model expressing mutant ATXN1 only in Purkinje cells. We found no changes in cell numbers in the SCA1 cerebellum. We validated previously indicated pathway and gene expression changes in the Purkinje cells, and identified novel DEG and pathways in Purkinje cells, including *Ralyl* that may provide compensatory roles and maintain PC function. Importantly we identified profound non-cell autonomous and potentially neuroprotective gene expression and pathway alterations in Bergman glia, velate astrocytes and oligodendrocytes that may contribute to disease pathogenesis.

Introduction

Glia cells play key roles required for the normal brain function [1]. These roles include maintaining homeostasis of ions, neurotransmitters and water, providing neurotrophic and energy support, removal of unused synapses, and fast propagation of neuronal potentials [2]. In most if not all neurodegenerative diseases, glial cells undergo reactive gliosis, a process that includes molecular, morphological and functional changes [3][4]. These glial changes have been shown to play active role in the pathogenesis of neurodegenerative diseases [5][6]. In some situations, reactive gliosis can be beneficial and delay and ameliorate pathogenesis, but reactive glia have been also found to exacerbate pathogenesis [7][8][9][10]. The neuroprotective or toxic nature of reactive glial phenotypes likely depends on the stage of disease progression and the mechanism and intensity of signaling that leads to their activation.

Glia can be activated in response to distress signaling from neurons or other neural cells. In many neurodegenerative diseases a disease-causing genes and proteins are expressed in glial cell. Therefore, in these diseases glia can be also activated in response to the toxic effect of disease causing genes and proteins within the glial cells themselves. It is important to understand both glial cell –autonomous and non-cell-autonomous reactive responses, as well as how they interact to produce resulting glial phenotypes in disease. We propose that the way to start to address these questions is to reduce complexity and use disease models of neurodegeneration that express mutant proteins only in neurons to first understand the non-cell autonomous glial changes (that are in response to neuronal/neural distress and dysfunction).

Spinocerebellar ataxia type-1 (SCA1) is dominantly inherited neurodegenerative disorder caused by the abnormal expansion of CAG repeats in the *Ataxin-1* (*ATXN1)* gene [11]. Repeat expansions of 39 or more CAG repeats result in SCA1 disease with larger expansions leading to earlier onset and more severe symptoms [12]. Symptoms of SCA1 include loss of balance and coordination, swallowing and speech difficulties, impairments in cognition and mood, and premature death [13][14][15][16]. Selective neuronal vulnerability in different brain regions despite wide

expression of mutant proteins is a feature shared by many neurodegenerative diseases. In case of SCA1 cerebellar Purkinje cells (PCs) are most affected although mutant ATXN1 is expressed throughout the brain. While *Atxn1*-targeting antisense oligonucleotides (ASO) show promise in pre-clinical trials [17], there are currently no disease-modifying treatments available for SCA1 [18], underlying the need for increased understanding of pathogenesis and neuronal vulnerability in SCA1. Severe vulnerability of PCs in SCA1 is likely brought about by the combination of the toxic effects of mutant ATXN1 within PCs and the PCs microenvironment, including glial cells. In this respect it is important to note that glial cells in the cerebellum have a very distinct transcriptome compared to the glial cells in other brain regions [19][20]. Uniqueness of cerebellar glia gets even more pronounced during ageing. Yet while neurodegeneration associated glial gene expression changes have been studied intensively in the other brain regions, less is known about gene expression changes in cerebellar glia during neurodegeneration [21][4].

Moreover, there are several excellent SCA1 mouse models that exhibit Purkinje cell pathology and motor deficits. In transgenic *Pcp2- ATXN1[82Q]* line mutant ATXN1 is expressed only in Purkinje cells in the cerebellum. Thereby, this mouse model is well suited to investigate the non-cell autonomous glial changes in neurodegenerative disease (that are in response to neuronal/neural distress and dysfunction)[22].

We decided to focus our study on Bergmann glia, velate astrocytes and oligodendrocytes for the following reasons. Bergmann glia are a special type of astrocytes whose cell bodies reside in Purkinje cell layer surrounding the cell bodies of Purkinje cells. BG processes extend into the molecular layer alongside PCs dendrites enveloping PCs synapses where BG regulate concentration of ions and neurotransmitters [23]. We have previously shown that Bergmann glia (BG) undergo reactive gliosis in patients with SCA1 and in SCA1 mouse models [24][25][26]. Moreover, we have demonstrated that early in disease progression reactive astrogliosis has a beneficial role delaying onset and slowing the progression of SCA1 pathogenesis in the *Pcp2-ATXN1[82Q]* line [25]. Velate astrocytes are unique among brain astrocytes as they are significantly outnumbered by granule neurons with glia to neuron

ratio of ~ 0.2 while in the rest of the brain it can be up to 10. Cells of oligodendrocytes lineage are important for cerebellar development and motor learning [27][28]. Previous studies have found significant changes in the cerebellar white matter in SCA1 patients and in *Pcp2-ATXN1[82Q]* mice, indicating that oligodendrocytes may be affected in SCA1 [29][30]. Moreover, recent study found a decrease in oligodendrocyte (OL) numbers in human post-mortem samples from patients with SCA1 and altered expression of number of oligodendrocyte precursor cells (OPC)/OL genes in bulk RNA set from SCA1 knock-in mice $Atxn1^{154Q/2Q}$ line.

The bulk RNA sequencing has been useful for determining cerebellum-wide changes in the gene expression in mouse models of SCA1. However, bulk RNA sequencing precludes the detection of transcriptional changes at the single-cell level and is also confounded by the possible change in the proportion of cell types. Therefore to investigate molecular non-cell autonomous gene and pathways changes in cerebellar glia we have used single-nuclei RNA sequencing.

Materials and Methods

Mice

The creation of the *Pcp2-ATXN1[82Q]* mice was previously described [31]. We have backcrossed these mice onto C57BL/6 background for 10 generations. As CAG repeats are unstable and tend to shrink in mice we periodically sequence CAG region to evaluate number of repeats [32]. At the time of experiments the average number of CAG repeats in our colony was 71. Animal experimentation was approved by Institutional Animal Care and Use Committee (IACUC) of University of Minnesota and was conducted in accordance with the National Institutes of Health's (NIH) Principles of Laboratory Animal Care (86–23, revised 1985), and the American Physiological Society's Guiding Principles in the Use of Animals [33].

Nuclei isolation

Nuclei for RNA sequencing were isolated using detergent mechanical lysis protocol as previously described [34]. Briefly, frozen or fresh whole cerebellum was placed into 1.5mL tube with 500uL pre-chilled detergent lysis buffer [low sucrose buffer (LSB) (sucrose 0.32M, 10 mM HEPES, 5mM CaCl2, 3mM MgAc, 0.1mM EDTA, 1mM DTT) with 0.1% Triton-X] and tissue was homogenized using mechanical homogenizer. 40um strainer was placed over a pre-chilled 50mL tube and pre-wetted with 1ml LSB. 1mL of LSB was added to the tube containing the crude nuclei in the lysis buffer and mixed gently by pipetting (2-3 times). Crude nuclei prep was then passed over the 40uM strainer into the pre-chilled 50mL tube, washed with 1 ml LSB and centrifuged at 3200g for 10 minutes at 4C The pellet was resuspended in 3mL of LSB, gently swirling to remove the pellet from the wall to facilitate the resuspension and left on ice for 2 min. Suspension was transferred to an Oak Ridge tube and nuclei were homogenized in LSB for 15-30s, keeping the sample on ice. Using a serological pipette, 12.5mL of density sucrose buffer (sucrose 1M, 10 mM HEPES, 3mM MgAc, 1mM DTT) was layered underneath the LSB homogenate, taking care not to create a bubble that disrupts the density layer. Samples were then centrifuge at 3200g for 20 minutes at 4C and pelleted nuclei were resuspended in the resuspension solution (PBS, 0.4 mg/ml BSA, 0.2 U/µl RNAse inhibitor). Nuclei were filtered through a 40um pore-size strainer followed by a 30um and 20um pore-size strainers. Small sample of nuclei was pelleted and added to the slide with VectaShield with DAPI to verify single nuclei isolation under fluorescent microscope. The nuclear suspensions were processed by the Genomic Core at the University of Minnesota using 10X Chromium 3' GEX Capture to Library Preparation (Chromium Next GEM Single Cell 3 Reagent Kits v3.1 with Single Cell 3’ v3.1 Gel Beads and Chromium Next GEM Chip G).

Sequencing and analysis

Library quality control was performed using MiSeq system to estimate average numbers of nuclei per donor mouse. Then all nuclei from 6 donors were multiplexed and sequenced on two independent

runs on the Illumina NovaSeq platform, using 1 full lane of S4 chip each time. Sequencing depth ranges from ~41,000 to ~120,000 reads per nuclei. Raw, demultiplexed fastq files were analyzed by CellRanger (v5.0.1) using reference genome mm10 (refdata-gex-mm10-2020-A), with the option that allows alignment to un-spliced pre-mRNAs (--include-introns). The resulted gene count table per donor was analyzed with R (v4.1.0) package Seurat (v 4.0.4). If bi-modal distribution was observed for nFeature (number of detected genes) per nuclei for a donor, nuclei composing the lower range peak were excluded from downstream analysis. Cell type identification was accomplished with SingleR (v 1.6.1) using DropViz (PMID: 30096299) Cerebellum MetaCells reference.

For identified cell types of Bergmann Cells, Velate Astrocytes, Granule Neurons, Purkinje Neurons and Oligodendrocytes, edgeR (v 3.34.1) was used to test differential abundance between control and KI donors. For the same identified cell types, scran (v 1.20.1) was used to normalize the single cell expression matrix, followed by limma-trend (v 3.48.3) to test for differential gene expression. Sample batches were considered as an independent factor in the design matrix of the statistical test (design = ~ genotype + batch). P values were adjusted using Benjamini-Hockberg method. Differential gene expression was determined by an adjusted p values of 0.05. The lists of differentially expressed genes from different cell types were further analyzed for GO term enrichment using ClusterProfiler (v 4.0.5).

Visualization of the results was generated using various R packages, including Seurat, ClusterProfiler, enrichplot (v 1.12.2), and ggplot2 (v 3.3.5).

Immunofluorescent (IF) staining

IF was performed on a minimum of six different floating 45-µm-thick brain slices from each mouse (six technical replicates per mouse per region or antibody of interest). Confocal images were acquired using a confocal microscope (Olympus FV1000) using a 20X oil objective. Z-stacks consisting of twenty non-overlapping 1-µm-thick slices were taken of each stained brain slice per brain region (i.e., six z-stacks per mouse, each taken from a different brain slice). The laser power and detector gain

were standardized and fixed between mice within a surgery cohort, and all images for mice within a cohort were acquired in a single imaging session to allow for quantitative comparison.

We used primary antibodies against Myein Basic protein, and GFAP. To quantify relative intensity of staining we measured the average signal intensity in the region of interest and normalized it to that of the WT littermate controls.

Reverse transcription and quantitative polymerase chain reaction (RT-qPCR)

Total RNA was extracted from dissected mouse cerebella, medulla, and hippocampus using TRIzol (Life Technologies), and RT-qPCR was performed as described previously [8]. We used IDT Primetime primers for the following genes: *Ralyl*, *Mog*, *Ptch1*, *Ptch2*, *Gli* and *ApoE*. Relative mRNA levels were calculated using 18S RNA as a control and wild-type mice as a reference using $2^{-\Delta\Delta-Ct}$ as previously described.

Data availability

All the data from this study are available from the authors.

Results

Mutant ATXN1 expression in Purkinje cells does not lead to the significant change in proportions of cerebellar cells

This study aimed to address question how neuronal dysfunction affects glial cells in cerebellar neurodegeneration. To ensure that glial cells are affected solely in the non-cell autonomous manner we have used Purkinje cells specific transgenic mouse model of SCA1, *Pcp2-ATXN1[82Q]* mice [22]. In these mice mutant *ATXN1* with 82 CAG repeats is selectively expressed under *Purkinje cell protein 2 (Pcp2)* promoter in cerebellar Purkinje cells. Because repeat length in trinucleotide repeat expansions is unstable and prone to further expansion or shrinkage [32], we routinely perform genetic sequencing of our mouse lines. We found that the number of repeats has recently decreased in our colony from 82 CAG to 71 CAG. Despite this reduction in CAG number, expression of Purkinje cell

genes associated with SCA1 degeneration [35] remained significantly downregulated (**Supplementary Figure 1**).

Previous studies have shown advantages of single nuclei over single cell RNAseq. These include preservation of a larger number of cells across multiple subtypes, while minimizing the effects of cell dissociation on gene expression, and enriching for transcripts that are being actively transcribed *in vivo* [36][37]. Therefore we have performed RNA sequencing on isolated cerebellar individual nuclei that were captured and barcoded (**Figure 1A**)[38][39]. We isolated nuclei from the cerebella of six 12 weeks-old SCA1 and littermate control mice. We chose 12 weeks of age to capture the early stage when disease is still reversible [40] and as such therapeutically noteworthy. Bulk RNA seq showed significant gene expression changes in the cerebella at 12 weeks, yet there was no detectable PCs death [35][41].

We identified a total of 47894 high-quality, snRNAseq profiles. Debris-contaminated nuclei were removed with Seurat using cutoff on number of genes per nuclei or mitochondrial gene percentage, as well as using semi-supervised machine learning classifier Debris Identification using Expectation Maximization (DIEM)[42]. We classified nuclei into the cell types with SingleR (v 1.6.1) using DropViz Cerebellum MetaCells reference [43] (**Figure 1B**).

First, we wanted to determine whether there cellular composition of the cerebellum is altered in SCA1 e.g. whether expression of mutant ATXN1 in Purkinje cells leads to the relative increase or decrease in the numbers of the main cerebellar cell types, including Purkinje cells (PCs), Bergmann glia (BG), velate astrocytes (VA) and oligodendrocytes (OL).

We calculated the percentage of each cell type by dividing the number of specific cell type by the total number of nuclei. As expected majority of the cerebellar nuclei were classified as granule neurons (80.75%). We have not found statistically significant difference in the relative percentages of granule neurons, Purkinje cells, Bergmann glia, velate astrocytes and oligodendrocytes in *Pcp2-ATXN1[82Q]* and wild-type mice, indicating that at this early disease stage we cannot detect a change in the cerebellar cell type composition in *Pcp2-ATXN1[82Q]* mice (**Figure 1C**).

Expression of mutant ATXN1 in Purkinje cells causes significant gene expression changes in cerebellar glia

Most gene expression studies so far were focused on understanding how mutant ATXN1 affects PCs. Here we extended the analysis of SCA1 gene expression changes to Bergmann glia (BG), velate astrocytes (VA) and oligodendrocytes (OL) in addition to Purkinje cells (PCs) in 12 week old *Pcp2-ATXN1[82Q]* mice [44].

Using differential gene expression analysis we identified differentially expressed genes (DEGs) for each of these four cell types. We found that different cell types have different numbers of DEGS (**Figure 1D)**. Remarkably, Bergmann glia and Purkinje cells had a comparable number of DEGs (575 and 406 respectively) at 12 weeks despite the fact that mutant ATXN1 is expressed only in Purkinje cells in these mice. This significant non-cell autonomous transcriptional alterations in Bergmann glia, may suggest that BG are highly sensitive to perturbation in PCs. Both velate astrocytes and oligodendrocytes had a significant number of DEGs (157 and 155 respectively, **Figure 1D)**. These results indicate that ATXN1 induced dysfunction in Purkinje cells significantly affects not only nearby Bergmann glia, but also velate astrocytes and oligodendrocytes in a non-cell autonomous manner.

Molecular profiling of Purkinje cells confirms previously identified molecular pathways and identifies potentially compensatory genes

We compared gene expression changes in PCs to previously reported transcriptional alterations [45][46]. We identified 575 DEGs in Purkinje cells (p.adj $q < 0.05$), 56% of which were downregulated and 44% upregulated (**Figure 2A**). This prevalence of downregulated genes is consistent with previous results and is generally thought to reflect the cell-autonomous repressive effect of mutant ATXN1 on transcription in PCs [46].

Among top ten upregulated genes were *Heparan Sulfate 6-O-Sulfotransferase 3* (*Hs6st3*), *Adhesion G Protein-Coupled Receptor L3* (*Adgrl3*), *Contactin 5* (*Cntn5*), and *Neuregulin 1* (*Nrg1*) known for their roles in neurodevelopment [47][48][49][50]. In addition, SCA1 PCs had increased expression of *RALY RNA Binding Protein-like (Ralyl)* known as Alzheimer's disease cognitive reserve gene [51] (**Figures 2A-C**). Among upregulated genes were also three vacuolar V-type ATP-ase subunits (*Atp6v0c*, *Atpgv0a1*, and *Atp6v1h*) and *Slc32a1*, encoding vesicular GABA and Glycine Transporter (VGAT) indicating that synaptic vesicles SCA1 PCs may have increased GABA content. These genes may represent compensatory increases in PCs gene expression to restore, or ameliorate synaptic transmission.

Among ten most downregulated genes are four Magenta module genes (*Fam 107b*, *Trabd2b* (regulator of Wnt signaling), *Anks1b*, and *Atl 2)*, three genes encoding extracellular matrix proteins (*Muc3a*, *Col5a1*, *Col 18a*), and two genes encoding proteins involved in GPCR signaling (phosphodiesterase *Pde10* and G protein coupled receptor *Lgr5* that regulates Wnt signaling). Downregulated genes encode calcium voltage gated channels Cav2.1 and Cav3.1 (*Cacna1a, Cacna2d2,* and *Cacna 1g*), calcium endoplasmatic reticulum pumps SERCA1 and SERCA2 (*Atp2a2* and *Atp2a3*), ionotropic glutamate receptors (*Gria2, Gria3, Grid2* associated with Spinocerebellar ataxia autosomal recessive 18, *Grid2ip, Grin2a)*, and potassium channels (*Kcnc3*, associated with SCA13, and *Kcnab1,* associated with Episodic Ataxia Type 1*)*[52] (**Figures 2C-D**).These results are consistent with previous studies implicating ion channel, calcium and potassium dysregulation and synaptic dysfunction in SCA1 [53].

It is important to note that for most genes, expression in PCs does not seem to be uniform, as indicated by the heatmap and histograms (**Figures 2 C-D)**.

Previous studies used weighted Gene Coexpression Network Analysis of the cerebellar bulk RNAsequencing data from *Pcp2-ATXN1[82Q]* mice to identify Magenta Module as a gene network that is significantly correlated with disease progression in Purkinje cells [46]. Thus the Magenta Module is thought to provide a signature of suppressed genes that reflect disease progression in

Purkinje cells. We examined which of the Magenta Module genes are changed in Purkinje cells in our single nuclei gene expression analysis. Out of 342 magenta genes Allen brain atlas suggested that 94 (27%) are PC enriched, 175 (51%) PC exclusive and 31 (9%) belonging to multiple cells lines [46]. In previous studies not all of the Magenta Module genes were found to be significantly altered at 12 weeks in *Pcp2-ATXN1[82]* mice. Indeed we found that in our data 103 (30.1%) of Magenta Module genes are altered at 12 weeks of age in *Pcp2-ATXN1[82]* mice. Of those 74 were altered only in PCs (71.8%), while 29 (28.2%) were also changed in two or more cell types, including Bergmann glia, velate astrocytes, and oligodendrocytes. Most intriguing were 13 Magenta Module genes that were changed in all four cell types (**Figure 2E**). For instance expression of gene encoding inositol 3 phosphate receptor 1 (ITPR1) that regulates calcium release from the ER, *Pcp4,* encoding Purkinje Cell Protein 4 that regulate calcium binding to calmodulin, and *Gng13* encoding G Protein Subunit Gamma 13, regulating G protein coupled receptor signaling were significantly suppressed in many cerebellar cell types. This indicates that calcium and G protein signaling are altered not only in PCs, but also in BG, VAs, and OLs. On the other hand expression of *Dner*, encoding for Delta/Notch Like EGF Repeat Containing seems to be altered mostly in cerebellar neurons including PCs, Basket cells, golgi neurons and unipolar brush cells. *Dner* has been previously found to be an important component of PC-BG communication and cerebellar function as expression of DNER in Purkinje cells induces morphological differentiation and functional maturation of Bergmann glia and loss of *Dner* impairs motor behavior of mice [54][55]. It is unclear what role Dner plays in other cerebellar neurons. Pathway analysis of downregulated DEGs using Gene ontology (GO) identified calcium binding ($q = 9.8 \times 10^{-3}$), and dendrite and dendritic tree (q values of 1.45 and 1.48×10^{-5} respectively), while top Kyoto Encyclopedia of Genes and Genomes (KEGG) pathways of downregulated genes were long-term depression ($q = 4.9 \times 10^{-4}$), cholinergic ($q = 3.2 \times 10^{-3}$), glutamatergic ($q = 3.3 \times 10^{-3}$), serotoninergic ($q = 5.2 \times 10^{-3}$) and dopaminergic ($q = 5.5 \times 10^{-3}$) synapse and retrograde endocananbinoid signaling ($q = 7.1 \times 10^{-3}$) consistent and building up on the previous studies.

Hierarchical enriched pathways analysis of both up and downregulated genes identified many pathways involved in synapse function including synapse organization, cell junction assembly, locomotory behavior, regulation of synapse structure or activity, synapse assembly, and regulation of neurotransmitter levels (**Figure 2F**). Among top GO pathways associated with the upregulated genes were synapse assembly ($q = 3.42 \times 10^{-4}$), synaptic membrane adhesion ($q = 6.1 \times 10^{-4}$), cell junction assembly ($q = 8.8 \times 10^{-4}$), synapse organization ($q = 3.2 \times 10^{-3}$) and cell junction organization ($q = 8.1 \times 10^{-3}$). Kyoto Encyclopedia of Genes and Genomes (KEGG) identified axon guidance ($q = 1.4 \times 10^{-5}$) and synaptic vesicle cycle ($q = 2.9 \times 10^{-3}$) as dysregulated pathways.

In conclusion, we confirmed changes in ion transport and synapse dysfunction in SCA1 Purkinje cells as well as identified novel genes that may provide compensatory roles, including *Ralyl*.

Molecular profiling points to disruptions of multiple pathways in Bergmann glia including Sonic hedgehog signaling from Purkinje cells

Bergmann glia are intimately connected with Purkinje cells with BG cell bodies surrounding the cell bodies of PC and BG radial processes lining up next to PC dendrites and enveloping their synapses in the molecular layer. BG are essential for PCs function and viability through their many roles including maintenance of potassium homeostasis, removal of synaptic glutamate and neurotrophic support [56][57][58][59][60]. Similarly, PCs signaling is important for the development and maintenance of Bergmann glia character [54] [44]. With both their soma and processes next to each other, BG are perfectly poised to sense and respond to PC dysfunction including caused by mutant ATXN1 in SCA1.

We identified 406 DEGs (p.adj <= 0.05) in Bergmann glia. Out of these 151 (37.2%) were downregulated and 255 (62.8%) upregulated (**Figure 3A**). As previous studies indicated that mutant ATXN1 leads to inhibition of gene expression, the increased ratio of upregulated to downregulated

genes in BG compared to the opposite ratio in PC, is consistent with the idea of non-cell autonomous gene expression changes in BG.

Among the top upregulated BG genes were transthyretin (*Ttr*) that encodes for the transporter of vitamin A (retinol). Retinol is important for cerebellar function [61] and previous studies found that it is implicated in SCA1 [62]. In addition, BG have increased expression of calmodulin regulated adenylate cyclase (*Adcy8*), that is implicated in Alzheimer's disease astrocytes and important for memory [63][64], long non coding RNA (lncRNA) *Rmst* that aids in the function of Sox2 transcription factor that is required for BG function [65][66], and *Cystatin* (*Cst3*), the most abundant extracellular inhibitor of cysteine proteases that is thought to be neuroprotective in neurodegenerative diseases[67][68]. We have also found increased expression of *Aquaporin4* (*Aqp4*) that regulates water homeostasis [69] and *Kcnj3*, potassium rectifying channel Kir3.1, that could also be neuroprotective in SCA1. Expression of several trophic factors including fibroblast growth factor (*FGF) 12*, and *Platelet Derived Growth Factor D (PDGFD)* is also increased in BG. Among the upregulated genes was *glial fibrillary acidic protein* (*Gfap*). Additionally, expression of secreted protein acidic and rich in cysteine like 1 (SPARCL1) that directly promotes excitatory synapse formation is increased and is likely compensatory to decreased number of excitatory VGLUT2 synapses on PCs seen at this stage of disease [25]. As increased *Gfap* is thought to reflect during reactive gliosis these BG gene expression changes may implicate increased neuroprotective functions of reactive BG induced by PC dysfunction. (**Figure 3B-C)**.

We found a significant changes in the expression of genes involved in homeostatic BG roles that are key for PC neuronal function (**Figure 3D**). Expression of *Kcnj10*, encoding the potassium inward rectifier Kir4.1 is decreased in BG at this stage of disease. Previous studies have found that reduced expression of *Kcnj10* is sufficient to cause PC dysfunction and ataxia in mice [57]. Moreover expression of *Solute carrier family 1 Member 3 (Slc1a3)* that encodes for the glutamate transporter Glast that is key to remove synaptic glutamate is also decreased in BG [70]. These results indicate that SCA1 BG may be less effective in performing these important homeostatic functions.

We also found a large decrease in the expression of inositol tri phosphate receptor 1 (IP3R1), receptor on the ER that upon binding IP3 binding leads to the calcium influx into cytosol [71], that may affect BG function.

Previous studies have found that PC regulate BG character via Sonic hedgehog (Shh) signaling [72]. Expression of Shh receptors *Patched 1 and 2* (*Ptch1, Ptch2*)[73] is decreased in BG in *Pcp2-ATXN1[82Q]* cerebella indicating one critical way in which PC-BG communication is impacted in SCA1 that could affect their function including reduced expression of *Kcnj10* and increased expression of *Aqp4*. Expression of Shh downstream transcriptional activator *Gli1* is also decreased, further supporting dysfunctional Shh PC-BG signaling in SCA1 (**Figure 3D**).

Hierarchical enriched pathways analysis identified pathways involved in development, including cell junction assembly, positive regulation of cell projection organization, regulation of neurogenesis, axonogenesis, gliogenesis, small molecule metabolic processes and neuron apoptotic processes (**Figure 3E**). Among top GO pathways associated with the upregulated genes were nervous system development ($q = 1.2 \times 10^{-9}$), regulation of biological quality ($q = 1.5 \times 10^{-9}$), cell adhesion ($q = 9.8 \times 10^{-9}$), organonitrogen compound metabolic processes ($q = 3.8 \times 10^{-7}$) and cell projection organization ($q = 5 \times 10^{-8}$). KEGG identified circadian entrainment ($q = 3.6 \times 10^{-2}$) as dysregulated pathway in BG. This is very intriguing considering the role of cerebellum in sleep and sleep disturbances in SCA patients[74][75]. Go pathway analysis of downregulated genes identified transmembrane transporter binding ($q = 7 \times 10^{-3}$), smoothened binding and hedgehog receptor activity ($q = 4.9 \times 10^{-2}$), cell cell signaling ($q = 6.4 \times 10^{-7}$), apoptotic processes ($q = 1.3 \times 10^{-2}$) and synapse ($q = 5 \times 10^{-14}$). KEGG analysis of downregulated genes identified retrograde endocannabinoid signaling ($q = 1 \times 10^{-3}$), glutamatergic ($q = 2 \times 10^{-3}$) and dopaminergic synapses ($q = 4.3 \times 10^{-2}$), long-term depression ($q = 8.1 \times 10^{-3}$) and spinocerebellar ataxias ($q = 8.4 \times 10^{-3}$). Thus pathway analysis further supports that SCA1 BG increase their neuroprotective functions to compensate for PC dysfunction, but they decrease their homeostatic roles that may promote PC dysfunction. This decrease in the expression

of homeostatic genes may be in part due to reduced ability to receive Shh signaling from PC due to the reduced expression of *Ptch1* and *Ptch2*.

Increased expression of genes to promote neurogenesis, gliogenesis and synaptogenesis indicate beneficial compensatory gene expression changes in velate astrocytes

Velate astrocytes are type of cerebellar astrocytes that reside in the granule cell layer. As such they are surrounded by the most numerous neurons in the brain and are the only astrocytes in the brain that are largely outnumbered by neurons [76]. Moreover while volume of the whole cerebellum is reduced in SCA1, much less is known about the pathology in granule cell layer.

We have identified 157 DEGs (p.adj <= 0.05) in SCA1 velate astrocytes compared to their wild-type littermate controls with 114 or 72.6% of genes upregulated (**Figure 4A, D**). One of genes with increased expression was *Vimentin* (*Vim*) encoding for the intermediate filament predominantly found in astrocytes and upregulated when they are undergoing reactive astrogliosis [77][78]. This result may indicate that VA undergo reactive gliosis in SCA1 (Figure 4D). Expression of *apolipoprotein E* (*ApoE*) was also significantly increased in SCA1 velate astrocytes. As ApoE, among other roles contributes to astrocyte activation and BDNF secretion, this increase in ApoE may contribute to VA activation and increased BDNF early in SCA1. [79][80]. Among the top upregulated genes was *Transthyretin* (*Ttr*), encoding for protein primarily responsible for the transport of thyroxin and retinol-retinol binding complex (RBP-complex) but also plays a role in oxidative stress [81]. Moreover increased expression of *Ttr* is suggested to play a role in resistance to AD neurodegeneration [82]. *Neural Cell adhesion molecule 2* (*Ncam2*) encodes NCAM2 protein that is involved in neuronal migration, cell positioning during corticogenesis, neuronal differentiation and synaptogenesis during development and in the calcium signaling, maintenance of presynaptic and postsynaptic compartments in adult brains. In addition, it has been proposed that a decrease in NCAM2 levels is associated with loss of structure of synapses in the early stages of neurodegenerative diseases [83]. Recently, *CUB And Sushi Multiple*

Domains 1(*Csmd1*) was suggested to oppose the complement cascade that facilitates synaptic loss in neurodegeneration[84]. Therefore, it is reasonable to assume that increased expression of *ApoE*, *Ttr*, *Ncam2*, and *Csmd1* may be neuroprotective in SCA1 as well.

Most of the homeostatic astrocytic genes were not altered with the exception of reduced expression of *vascular endothelial growth factor* (*VEGF)*, neurotrophic factor whose decrease was previously shown to contribute to Purkinje cell pathology in SCA1 [85] and genes encoding astrocyte receptors *Itpr1* and *G Protein Subunit Gamma 13* (*Gng13*), that regulate calcium and GPCR signaling were downregulated (**Figure 4D**).

Finally, we examined the expression of A1 and A2 astrocyte genes in VA and BG. Previous study identified two different types of reactive astrocytes that were termed “A1” and “A2” respectively. A1 astrocytes are thought to be harmful as they up-regulate classical complement cascade genes previously shown to be destructive to synapses, while A2 astrocytes are thought to be neuroprotective due to increased expression of neurotrophic factors. We found increased expression of panreactive genes Gfap, Vim, and CD44 but have not found any clear pattern or distinction in the expression of A1 or A2 genes (**Figure 4E**)

Pathways analysis identified developmental pathways including regulation of neurogenesis, gliogenesis, positive regulation of projection organization, regulation of nervous system development as well as, regulation of protein catabolic process (**Figure 4F)**.

Pathway analysis of the upregulated identified many developmental pathways including cell morphogenesis, regulation of neuron projection development, positive regulation of gliogenesis, and glial differentiation (q values of 3.2 $X10^{-6}$, 1.5 $X10^{-5}$, 3.9 $X10^{-5}$, and 4.5 $X10^{-5}$ respectively).

Pathway analysis of the downregulated genes identified calcium ion binding (q = 3.1 $X10^{-3}$), vesicle mediated transport in synapse (q = 3.5 $X10^{-2}$), negative regulation of neuronal death (q = 4.1 X 10^{-2}), glutamatergic synapse (q = 4.5 $X10^{-4}$), spinocerebellar ataxia (q = 1.3 $X10^{-3}$) , retrograde endocannabinoid signaling (q = 2.4 $X10^{-2}$), and long-term depression (q = 2.7 $X10^{-2}$).

Gene expression analysis indicates reactive activation and perturbation in calcium homeostasis in SCA1 oligodendrocytes while pathways analysis revealed association with locomotor behavior and cognition

Oligodendrocytes (OL) envelop axons with myelin and maintain long-term axonal integrity [86]. Previous studies demonstrated atrophy in white matter already present in pre-manifest carriers of SCA1 mutation [29] as well as in *Pcp2-ATXN1[82Q]* mice [30]. These studies indicated functional changes in oligodendrocytes in SCA1 from the early stages of disease progression. Moreover recent sn-RNAseq study indicated decreased expression of mature oligodendrocyte genes, including *Myelin Oligodendrocyte Glycoprotein* (*Mog*) and oligodendrocyte precursor (OPC) genes involved in OL formation in a knock-in mouse model of SCA1, *Atxn1*$^{154Q/2Q}$ mice. In *Atxn1*$^{154Q/2Q}$ mice mutant Atxn1 is expressed widely. To gain insight into which of these genes are induced in response to PC pathogenesis, we examined genes and pathways altered in oligodendrocyte nuclei from *Pcp2-ATXN1[82Q]* mice compared to littermate controls.

We found 154 DEGs in oligodendrocytes in *Pcp2-ATXN1[82Q]* cerebella, with majority (94 DEG or 61%) of genes being upregulated (**Figure 5A**).

While OL numbers are not altered, expression of several oligodendrocyte marker genes including *Transferrin* (*Trf)*, *Mog*, *Claudin 11* (*Cldn11*) and *Reticulon 4* (*Rtn4*) was increased (**Figures 5B-D**)[86].

We found altered expression of many genes important for oligodendrocyte function (Figure 5E). Among them is increased expression of *Glutamate-Ammonia Ligase* (*Glul*) encoding for glutamine synthetase (GS) a key enzyme that catalyzes the conversion of glutamate to glutamine. Previous studies demonstrated that OL glutamine synthetase is important for glutamatergic transmission [87], and that *Glul* expression in OL is increased in chronic pathological conditions including amyotrophic lateral sclerosis (ALS) and multiple sclerosis (MS)[88]. We also found increased expression of *Crystallin Alpha B* (*Cryab*) and *ApoE* in SCA1 OL. Increased *Cryab* and *ApoE* have been associated

with protective effects and astrocyte gliosis in other neurodegenerative diseases including Parkinson's disease (PD), Alzheimer's disease (AD) and MS [89][90][91][92][80]. Increased expression of transcriptional factor *JunD*, a functional component of activated protein 1 (AP1) complex that regulates many of the inflammatory and immune genes, also indicates reactive SCA1 OL response in pathogenesis [93].

Among downregulated genes were *Atp2a2* and *Atp2a3* encoding for calcium endoplasmatic reticulum pumps SERCA1 and SERCA2, *Atp2b2* encoding for Plasma Membrane Calcium-Transporting ATPase, and *Itpr1* implicating perturbation in calcium homeostasis in reactive SCA1 OLs (**Figures 5 B-D**).

Intriguingly top two pathways identified were cognition and locomotor behavior, implicating that molecular pathway alterations in SCA1 oligodendrocytes are associated with the changes in cognition and locomotion in these mice. Pathway analysis also identified regulation of neurotransmitter levels, positive regulation of synaptic transmission, vesicle- mediated transport in synapses and neurotransmitter secretion potentially implicating OL in alterations of synaptic transmission in SCA1 (**Figure 5E**).

Pathway analysis of downregulated genes identified pathways involved in transport and binding of ions including inorganic cation transmembrane transporter activity ($q = 7.5 \times 10^{-6}$), calcium binding ($q = 9.3 \times 10^{-6}$), P-type calcium transporter activity ($q = 4.2 \times 10^{-4}$), synaptic signaling including synaptic signaling ($q = 1.6 \times 10^{-7}$), modulation of chemical synaptic transmission ($q = 5.4 \times 10^{-6}$), glutamatergic synapse ($q = 6.4 \times 10^{-6}$), and Spinocerebellar ataxia ($q = 2.9 \times 10^{-5}$). Among the pathways identified with upregulated genes were movement of cell or subcellular component ($q = 9.4 \times 10^{-5}$), cell migration ($q = 8.8 \times 10^{-4}$), myelin sheath ($q = 2.4 \times 10^{-7}$), synapse ($q = 1.4 \times 10^{-4}$), Parkinson's disease ($q = 4.6 \times 10^{-3}$), and iron uptake and transport ($q = 3.8 \times 10^{-2}$).

Discussion

Here, we have employed single nuclei RNA sequencing to investigate transcriptional changes in individual cerebellar cell types during the early stages of disease progression in transgenic Purkinje cell specific mouse model of SCA1 *Pcp2-ATXN1 [82Q]* line. These results provide insight into how pathogenic processes within neurons, in this case Purkinje cells, affect gene expression and signaling pathways within cerebellar astrocytes and oligodendrocytes increasing our understanding of the causal sequences of progressive dysfunctions during early stages of disease.

There are several important findings from our study. First, mutant ATXN1 expression in Purkinje cells causes profound transcriptional alterations in cerebellar glia in a non-cell autonomous manner. Majority of the altered glial genes were upregulated (Bergmann glia (62.8%), velate astrocytes (72.6%) and oligodendrocytes (61%)). On the other hand mutant ATXN1 primarily caused downregulation of gene expression in cell autonomous manner in PCs as 56% of genes had reduced expression [94]. At 12 weeks there is no Purkinje cell loss in *Pcp2-ATXN1[82Q]* so we propose that these glial transcriptome changes are in response to Purkinje cell dysfunction [46]. In addition, we found that proximity to dysfunctional neurons seems to be an important factor in determining the extent of the glial non-cell autonomous transcriptional perturbations in SCA1. Bergmann glia that reside next to Purkinje cells have similar number of DEGs as Purkinje cells themselves and approximately three times more DEGs than velate astrocytes and oligodendrocytes that reside further away from PCs. This finding supports the previous evidence of very intimate relationship between PCs and BG [95].

Second, we identified transcriptional changes in PCs, BG, VA and OL that may be relevant to disease pathogenesis. For PCs we validated the findings from previous studies but also identified novel, potentially compensatory gene expression changes such as increased expression of *Ralyl*, *Atp6v0c*, *Atpgv0a1*, *Atp6v1h*, Atp6v and *Slc32a1. Ralyl* is an RNA binding protein known for its neuroprotective role in Alzheimer's [51]. Increased expression of three vacuolar V-type ATP-ase subunits (*Atp6v0c*,

Atpgv0a1, and *Atp6v1h*) that provide electrochemical gradient to fill synaptic vesicles with GABA and *Slc32a1*, encoding vesicular GABA and Glycine Transporter (VGAT) that transports GABA in the vesicles may suggest increased GABA content in PCs synaptic vesicle. As spontaneous firing rate of PCs is decreased in *Pcp2-ATXN1[82Q]* mice [96], this increase in GABA per vesicle may represent compensatory change to restore, or ameliorate synaptic transmission by increasing the amount of GABA released at PC terminals.

We validated previously reported decrease in the expression of glutamate transporter *Slc1a3* in Bergmann glia [70], and identified additional perturbations in the expression of homeostatic genes such as *Kcnj10* that are critical for PC function [97][57]. Moreover, our results suggest perturbed Shh signaling as one possible mechanism of these BG molecular alterations. Sonic hedgehog (Shh) signaling is one of the key communication pathways between PCs and BG involved in regulation of BGs character by PCs [72]. We found that the expression of Shh receptors Patched 1and 2 is decreased in BGs. Moreover, the expression of Shh signaling downstream transcription factor Gli1 is also reduced on SCA1 BG. Previous studies have shown that SHH-Ptch2 communication regulates expression of homeostatic genes *Slc1a3*, *Kcnj10*, and *Aqp4* in Bergmann glia [44]. Therefore it is possible that decreased Shh signaling contributes to reduced expression of S*lc1a3* and *Kcnj10* and increased expression of *Aqp4* that we found in SCA1 BG. Thus reduced PC-BG communication via Shh signaling may impair expression of BG identity genes and their ability to support Purkinje cells by maintaining homeostasis of potassium, glutamate and water, leading to progressive cerebellar dysfunctions.

In velate astrocytes we identified increased expression of several genes such as *ApoE, Ncam2*, and *Csmd1* that may provide neuroprotection. For instance we have previously demonstrated that BDNF provides neuroprotection in SCA1 [98][99]. As ApoE, among other roles contributes to astrocyte activation and BDNF secretion, this increase in ApoE may contribute to VA activation and increased BDNF that we have seen early in SCA1 [79][80]. *Ncam2* and *Csmd1* are protective against loss of

synapses [83][84], and increase in their expression in SCA1 VA may ameliorate loss of synapses seen in SCA1.

Perhaps most intriguing are the transcriptional changes we identified in oligodendrocytes. While OL numbers do not seem to be altered at 12 weeks, we have found increased expression of OL marker genes and genes indicating OL reactive activation including *Trf*, *Mog*, *Cldn11*, *Rtn4*, *JunD, Cryab* and *ApoE*.

Third, we identified shared DEGs and pathways that are altered in all four cell types in SCA1. These shared pathways are involved in regulation of synapses, cytoarchitecture, calcium and development. For instance several magenta genes and Ttr are altered in PCs, BG, VA and OL. Transthyretin (Ttr) is a protein that binds and distributes thyroid hormones and retinol. Previous studies identified the importance of retinol in PC pathogenesis in SCA1 [62]. Moreover, recent studies found that it plays in regulation of OPCs proliferation and survival [100], described it as regulator of the δ-GABAA-R expression in cerebellar granule neurons [101] and regulator of glycolysis in astrocytes [102]. Therefore increased Ttr expression could be beneficial for many cerebellar cell types in SCA1. It will be important to understand the mechanism of *Ttr* upregulation in different cerebellar cell types and which cells are affected by increased *Ttr* in SCA1 cerebella. In addition, several Magenta genes, including genes involved in calcium homeostasis, such as *Atp2a2* and *Itpr1* are reduced in all four cell types, indicating that calcium signaling may be altered in SCA1 PCs, BG, VA and OL. Identification of shared DEGs and pathways indicate that in response to the neuronal dysfunction neurons and glial cells undergo similar perturbations early in disease progression, prior to manifestation of motor symptoms. Thus these shared pathways may be ideal targets for therapeutic approaches.

It is likely that some of the molecular changes we identified are compensatory allowing for continued cerebellar function, and that some may be pathogenic, promoting disease progression. Our results provide a framework to investigate how individual pathogenic processes contribute to the sequence of progressive cerebellar dysfunctions in SCA1. Our results are freely available and we hope that they

will stimulate future studies to causally investigate how these gene and pathway perturbations contribute to SCA1 pathogenesis as well as facilitate development of novel therapeutic approaches.

Acknowledgements:

We acknowledge all the members of Orr and Cvetanovic laboratories for thoughtful discussions and feedback on the study. Work in this study was aided by the Single Cell Services of the University of Minnesota Genomics Center.

Funding:

This work was supported by a National Institute of Health NINDS awards (R01 NS107387 and NS109077 to M.C.)

Author Contributions:

M.C. conceptualized the study. E.B. performed experiments. Y.Z. and M.C. analyzed data. M.C., E.B. and YZ wrote the manuscript.

Conflicts of Interest:

The authors report no conflicts of interest.

Figure legends

Figure 1. Experimental schematics, cell composition and DEGs per cell type in *Pcp2-ATXN1[82Q]* mice. A. Nuclei were isolated from the cerebella of 12 weeks old *Pcp2- ATXN1[82Q]* mice and wild-type littermate controls (N=3 of each). After passing library QC nuclei were sequenced on Illumina NovaSeq platform. **B.** Average percentages of Purkinje cells (PC), Bergman Glia (BG), velate astrocytes (VA), and oligodendrocytes in p*cp2- ATXN1[82Q]* mice and wild-type littermate controls (N=3 of each). **C.** Number of differentially expressed genes in each cell type.

Figure 2. Single nuclei analysis identifies SCA1 disease associated transcriptional changes in Purkinje cells. A. Number of upregulated and downregulated DEGs in PCs. **B**. Volcano plot of PCs DEGs **C.** Heatplot of 25 highest upregulated and downregulated PC DEGs. **D.** Ridgeplot showing expression of selected PC DEGs. **E**. Differential expression of Magenta genes in different cerebellar cell types. **F.** Pathway Analysis

Figure 3. Mutant ATXN1 causes significant non-cell autonomous gene expression perturbations in SCA1 Bergmann glia. A. Number of upregulated and downregulated DEGs in BG. **B**. Volcano plot of BG DEGs **C.** Heatplot of 25 highest upregulated and downregulated BG DEGs. **D.** Ridgeplot showing expression of selected BG DEGs. **E**. Pathway Analysis

Figure 4. Velate astrocytes gene expression changes in SCA1. A. Number of upregulated and downregulated DEGs in VA. **B**. Volcano plot of VA DEGs **C.** Heatplot of 25 highest upregulated and downregulated VA DEGs. **D.** Ridgeplot showing expression of selected VA DEGs. **E**. Heatplot showing expression of A1/A2 genes in BG and VA. **F.** Pathway Analysis

Figure 5. Gene expression changes in SCA1 oligodendrocytes. A. Number of upregulated and downregulated DEGs in OL. **B**. Volcano plot of OL DEGs **C.** Heatplot of 25 highest upregulated and downregulated OL DEGs. **D.** Ridgeplot showing expression of selected OL DEGs. **E**. Pathway Analysis

Supplementary Figure 1. Pathway analysis of Magenta Module genes altered in PCs, BG, VA and OLs in *Pcp2-ATXN1[82Q]* mice.

Literature cited

1. Barres BA. The Mystery and Magic of Glia: A Perspective on Their Roles in Health and Disease. Neuron [Internet]. Elsevier Inc.; 2008;60:430–40. Available from: http://dx.doi.org/10.1016/j.neuron.2008.10.013

2. Perea G, Sur M, Araque A. Neuron-glia networks: integral gear of brain function. Front. Cell. Neurosci. [Internet]. 2014;8:378. Available from: http://www.pubmedcentral.nih.gov/articlerender.fcgi?artid=4222327&tool=pmcentrez&rendertype=abstract

3. Lobsiger CS, Cleveland DW. Glial cells as intrinsic components of non-cell-autonomous neurodegenerative disease. Nat Neurosci [Internet]. 2007;10:1355–60. Available from: http://www.ncbi.nlm.nih.gov/pubmed/17965655

4. Liddelow SA, Guttenplan KA, Clarke LE, Bennett FC, Bohlen CJ, Schirmer L, et al. Neurotoxic reactive astrocytes are induced by activated microglia. Nature [Internet]. Nature Publishing Group; 2017;541:481–7. Available from: http://dx.doi.org/10.1038/nature21029

5. Sheeler C, Rosa J, Ferro A, Mcadams B, Borgenheimer E, Cvetanovic M. Glia in Neurodegeneration□: The Housekeeper , the Defender and the Perpetrator. Int. J. Mol. Sci. 2020;21:1–16.

6. Yamanaka K, Chun SJ, Boillee S, Fujimori-Tonou N, Yamashita H, Gutmann DH, et al. Astrocytes as determinants of disease progression in inherited amyotrophic lateral sclerosis. Nat. Neurosci. 2008;11:251–3.

7. Qu W, Johnson A, Kim JH, Lukowicz A, Svedberg D, Cvetanovic M. Inhibition of colony-stimulating factor 1 receptor early in disease ameliorates motor deficits in SCA1 mice. J. Neuroinflammation. 2017;14:1–11.

8. Kim JH, Lukowicz A, Qu W, Johnson A, Cvetanovic M. Astroglia contribute to the pathogenesis of spinocerebellar ataxia Type 1 (SCA1) in a biphasic, stage-of-disease specific manner. Glia. 2018;66:1972–87.

9. Garden GA, Libby RT, Fu Y, Kinoshita Y, Huang J, Possin DE, et al. Polyglutamine-Expanded

Ataxin-7 Promotes Non-Cell-Autonomous Purkinje Cell Degeneration and Displays Proteolytic Cleavage in Ataxic Transgenic Mice. J. Neurosci. 2002;22:4897–905.

10. McLoughlin HS, Moore LR, Chopra R, Komlo R, McKenzie M, Blumenstein KG, et al. Oligonucleotide therapy mitigates disease in Spinocerebellar Ataxia Type 3 mice. Ann Neurol. 2018;84:64–77.

11. Orr HT, Chung MY, Banfi S, Kwiatkowski TJ Jr, Servadio A, Beaudet AL, McCall AE, Duvick LA, Ranum LP ZH. Expansion of an unstable trinucleotide CAG repeat in spinocerebellar ataxia type 1. Nat Genet. 1993;4:221.

12. Zoghbi HY, Orr HT. Pathogenic mechanisms of a polyglutamine-mediated neurodegenerative disease, Spinocerebellar ataxia type 1. J. Biol. Chem. 2009;284:7425–9.

13. Seidel K, Siswanto S, Brunt ERP, Den Dunnen W, Korf HW, Rüb U. Brain pathology of spinocerebellar ataxias. Acta Neuropathol. 2012;124:1–21.

14. I. K, M. M, T. S-H, M. H, T. K, U. W, et al. Neuropsychological features of patients with spinocerebellar ataxia (SCA) types 1, 2, 3, and 6. Cerebellum. 2010;9:433–42.

15. Zoghbi HY, Pollack MS, Lyons SLA, Ferrell TRE, Daiger SP, Beaudet AL. Spinocerebellar Ataxia□: Variable Age of Onset and Linkage to Human Leukocyte Antigen in a Large Kindred. Ann. Neurol. 1988;23:580–4.

16. Koeppen AH. The pathogenesis of spinocerebellar ataxia. The cerebellum. 2005;4:62–73.

17. Friedrich J, Henzler C, Orr HT, Friedrich J, Kordasiewicz HB, Callaghan BO, et al. Antisense oligonucleotide–mediated ataxin-1 reduction prolongs survival in SCA1 mice and reveals disease-associated transcriptome profiles. J. Clin. Investig. 2018;3.

18. Paulson HL, Shakkottai VG, Clark HB, Orr HT. Polyglutamine spinocerebellar ataxias-from genes to potential treatments. Nat. Rev. Neurosci. 2017.

19. Grabert K, Michoel T, Karavolos MH, Clohisey S, Baillie JK, Stevens MP, et al. Microglial brain region − dependent diversity and selective regional sensitivities to aging. Nat Neurosci. 2016;19:504.

20. Boisvert MM, Erikson GA, Shokhirev MN, Allen NJ. The Aging Astrocyte Transcriptome from

Multiple Regions of the Mouse Brain. Cell Rep. [Internet]. ElsevierCompany.; 2018;22:269–85. Available from: https://doi.org/10.1016/j.celrep.2017.12.039

21. Liddelow SA, Barres BA. Reactive Astrocytes: Production, Function, and Therapeutic Potential. Immunity [Internet]. Elsevier Inc.; 2017;46:957–67. Available from: http://dx.doi.org/10.1016/j.immuni.2017.06.006

22. Burright EN, Clark HB, Servadio a, Matilla T, Feddersen RM, Yunis WS, et al. SCA1 transgenic mice: a model for neurodegeneration caused by an expanded CAG trinucleotide repeat. Cell. 1995;82:937–48.

23. Bellamy TC. Interactions between Purkinje neurones and Bergmann glia. The cerebellum. 2006;5:116–26.

24. Cvetanovic M, Ingram M, Orr H, Opal P. Early activation of microglia and astrocytes in mouse models of spinocerebellar ataxia type 1. Neuroscience [Internet]. IBRO; 2015;289:289–99. Available from: http://linkinghub.elsevier.com/retrieve/pii/S0306452215000159

25. Kim JH, Lukowicz A, Qu W, Johnson A, Cvetanovic M. Astroglia contribute to the pathogenesis of spinocerebellar ataxia Type 1 (SCA1) in a biphasic , stage-of-disease specific manner. Glia. 2018;1–16.

26. Rosa J, Hamel K, Sheeler C, Borgenheimer E, Soles A, Ghannoum F, et al. Early stage of Spinocerebellar Ataxia Type 1 (SCA1) progression exhibits region- and cell-specific pathology and is partially ameliorated by Brain Derived Neurotrophic Factor (BDNF). BioRxiv. 2021;1:doi: https://doi.org/10.1101/2021.09.13.460129 ;

27. Mathis C, Collin L, Borrelli E. Oligodendrocyte ablation impairs cerebellum development. Development. 2003;130:4709–18.

28. McKenzie IA, Ohayon D, Li H, De Faria JP, Emery B, Tohyama K, et al. Motor skill learning requires active central myelination. Science (80-.). 2014;346:318–22.

29. Park YW, Joers JM, Guo B, Hutter D, Bushara K, Adanyeguh IM, et al. Assessment of Cerebral and Cerebellar White Matter Microstructure in Spinocerebellar Ataxias 1, 2, 3, and 6 Using Diffusion

MRI. Front. Neurol. 2020;11:1–13.

30. Liu CJ, Rainwater O, Clark HB, Orr HT, Akkin T. Polarization-sensitive optical coherence tomography reveals gray matter and white matter atrophy in SCA1 mouse models. Neurobiol. Dis. [Internet]. Elsevier; 2018;116:69–77. Available from: https://doi.org/10.1016/j.nbd.2018.05.003

31. Watase K, Weeber EJ, Xu B, Antalffy B, Yuva-Paylor L, Hashimoto K, et al. A long CAG repeat in the mouse Sca1 locus replicates SCA1 features and reveals the impact of protein solubility on selective neurodegeneration. Neuron. 2002;34:905–19.

32. Gatchel JR, Zoghbi HY. Diseases of unstable repeat expansion: mechanisms and common principles. Nat. Rev. Genet. 2005;6:743–55.

33. National Research Council (US) Committee for the Update of the Guide for the Care and Use of Laboratory Animals. Guide for the Care and Use of Laboratory Animals, 8th edition. 2011.

34. Matson KJE, Sathyamurthy A, Johnson KR, Kelly MC, Kelley MW, Levine AJ. Isolation of adult spinal cord nuclei for massively parallel single-nucleus RNA sequencing. J. Vis. Exp. 2018;2018:1–12.

35. Ingram M, Wozniak EAL, Duvick L, Zoghbi HY, Henzler C, Orr HT. Cerebellar Transcriptome Profiles of ATXN1 Transgenic Mice Reveal SCA1 Disease Progression and Protection Pathways Article Cerebellar Transcriptome Profiles of ATXN1 Transgenic Mice Reveal SCA1 Disease Progression and Protection Pathways. Neuron [Internet]. Elsevier Inc.; 2016;89:1194–207. Available from: http://dx.doi.org/10.1016/j.neuron.2016.02.011

36. Habib N, Avraham-Davidi I, Basu A, Burks T, Shekhar K, Hofree M, et al. Massively parallel single-nucleus RNA-seq with DroNc-seq. Nat. Methods. 2017;14:955–8.

37. Lacar B, Linker SB, Jaeger BN, Krishnaswami S, Barron J, Kelder M, et al. Nuclear RNA-seq of single neurons reveals molecular signatures of activation. Nat. Commun. 2016;7.

38. Klein AM, Mazutis L, Akartuna I, Tallapragada N, Veres A, Li V, et al. Droplet barcoding for single-cell transcriptomics applied to embryonic stem cells. Cell [Internet]. Elsevier Inc.; 2015;161:1187–201. Available from: http://dx.doi.org/10.1016/j.cell.2015.04.044

39. Zilionis R, Nainys J, Veres A, Savova V, Zemmour D, Klein AM, et al. Single-cell barcoding and sequencing using droplet microfluidics. Nat. Protoc. Nature Publishing Group; 2017;12:44–73.

40. Zu T, Duvick LA, Kaytor MD, Berlinger MS, Zoghbi HY, Clark HB, et al. Recovery from polyglutamine-induced neurodegeneration in conditional SCA1 transgenic mice. J. Neurosci. 2004;24:8853–61.

41. Mellesmoen A, Sheeler C, Ferro A, Rainwater O, Cvetanovic M. Brain derived neurotrophic factor (BDNF) delays onset of pathogenesis in transgenic mouse model of spinocerebellar ataxia type 1 (SCA1). Front. Cell. Neurosci. 2018;

42. Alvarez M, Rahmani E, Jew B, Garske KM, Miao Z, Benhammou JN, et al. Enhancing droplet-based single-nucleus RNA-seq resolution using the semi-supervised machine learning classifier DIEM. Sci. Rep. [Internet]. Nature Publishing Group UK; 2020;10:1–16. Available from: https://doi.org/10.1038/s41598-020-67513-5

43. Saunders A, Macosko EZ, Wysoker A, Brumbaugh S, Kulp D, Mccarroll SA, et al. Molecular Diversity and Specializations among the Cells of the Adult Mouse Brain Resource Molecular Diversity and Specializations among the Cells of the Adult Mouse Brain. Cell [Internet]. Elsevier Inc.; 2018;174:1015-1030.e16. Available from: https://doi.org/10.1016/j.cell.2018.07.028

44. Farmer WT, Chierzi S, Lui C, Zaelzer C, Jones E V, Bally BP, et al. Neurons diversify astrocytes in the adult brain through sonic hedgehog signaling. Science (80-.). 2016;351.

45. Serra HG, Byam CE, Lande JD, Tousey SK, Zoghbi HY, Orr HT. Gene profiling links SCA1 pathophysiology to glutamate signaling in Purkinje cells of transgenic mice. Hum. Mol. Genet. 2004;13:2535–43.

46. Ingram M, Wozniak EAL, Duvick L, Yang R, Bergmann P, Carson R, et al. Cerebellar Transcriptome Profiles of ATXN1 Transgenic Mice Reveal SCA1 Disease Progression and Protection Pathways. Neuron [Internet]. Elsevier Inc.; 2016;89:1194–207. Available from: http://linkinghub.elsevier.com/retrieve/pii/S0896627316001045

47. Mei L, Xiong WC. Neuregulin 1 in neural development, synaptic plasticity and schizophrenia. Nat.

Rev. Neurosci. 2008;9:437–52.

48. Moon S, Zhao Y-T. Spatial, temporal and cell-type-specific expression profiles of genes encoding heparan sulfate biosynthesis enzymes and proteoglycan core proteins. Glycobiology. 2021;31:1308–18.

49. Cocchi E, Fabbri C, Han C, Lee SJ, Patkar AA, Masand PS, et al. Genome-wide association study of antidepressant response: Involvement of the inorganic cation transmembrane transporter activity pathway. BMC Psychiatry [Internet]. BMC Psychiatry; 2016;16:1–12. Available from: http://dx.doi.org/10.1186/s12888-016-0813-x

50. El Hajj N, Dittrich M, Haaf T. Epigenetic dysregulation of protocadherins in human disease. Semin. Cell Dev. Biol. [Internet]. Elsevier Ltd; 2017;69:172–82. Available from: http://dx.doi.org/10.1016/j.semcdb.2017.07.007

51. Zhang Y, Wang J, Liu X, Liu H. Exploring the role of RALYL in Alzheimer's disease reserve by network-based approaches. Alzheimer's Res. Ther. Alzheimer's Research & Therapy; 2020;12:1–14.

52. Matsuda K, Matsuda S, Gladding CM, Yuzaki M. Characterization of the δ2 glutamate receptor-binding protein delphilin: Splicing variants with differential palmitoylation and an additional PDZ domain. J. Biol. Chem. [Internet]. Â© 2006 ASBMB. Currently published by Elsevier Inc; originally published by American Society for Biochemistry and Molecular Biology.; 2006;281:25577–87. Available from: http://dx.doi.org/10.1074/jbc.M602044200

53. Bushart DD, Shakkottai VG. Ion channel dysfunction in cerebellar ataxia. Neurosci. Lett. [Internet]. Elsevier; 2018;0–1. Available from: http://dx.doi.org/10.1016/j.neulet.2018.02.005

54. Eiraku M, Tohgo A, Ono K, Kaneko M, Fujishima K, Hirano T, et al. DNER acts as a neuron-specific Notch ligand during Bergmann glial development. Nat. Neurosci. 2005;8:873–80.

55. Tohgo A, Eiraku M, Miyazaki T, Miura E, Kawaguchi SY, Nishi M, et al. Impaired cerebellar functions in mutant mice lacking DNER. Mol. Cell. Neurosci. 2006;31:326–33.

56. Custer SK, Garden G a, Gill N, Rueb U, Libby RT, Schultz C, et al. Bergmann glia expression of polyglutamine-expanded ataxin-7 produces neurodegeneration by impairing glutamate transport. Nat.

Neurosci. 2006;9:1302–11.

57. Djukic B, Kristen B. Casper, Benjamin D. Philpot, Lih-Shen Chin and KDM. Conditional Knock-Out of Kir4.1 Leads to Glial Membrane Depolarization, Inhibition of Potassium and Glutamate Uptake, and Enhanced Short-Term Synaptic Potentiation. J. Neurosci. 2007;27:11354–65.

58. Rothstein J, Dykes-Hoberg M, Pardo C, Bristol L, Jin L, Kuncl R, et al. Antisense knockout of glutamate transporters reveals a predominant role for astroglial glutamate transport in excitotoxicity and clearance of extracellular glutamate. Neuron [Internet]. 1996;16:675–86. Available from: papers2://publication/uuid/327F682D-2D03-48C7-A0E6-A57E2CD92157

59. Miyazaki T, Yamasaki M, Hashimoto K, Kohda K, Yuzaki M, Shimamoto K, et al. Glutamate transporter GLAST controls synaptic wrapping by Bergmann glia and ensures proper wiring of Purkinje cells. Proc. Natl. Acad. Sci. [Internet]. 2017;114:7438–43. Available from: http://www.pnas.org/lookup/doi/10.1073/pnas.1617330114

60. Grosche J, Matyash V, Möller T, Verkhratsky A, Reichenbach A, Kettenmann H. Bergmann Glial AMPA Receptors Are Required for Fine Motor Coordination. Nat. Neurosci. [Internet]. 1999;2:139–43. Available from: http://www.ncbi.nlm.nih.gov/pubmed/10195197

61. Tafti M, Ghyselinck NB. Functional implication of the vitamin A signaling pathway in the brain. Arch. Neurol. 2007;64:1706–11.

62. Serra HG, Duvick L, Zu T, Carlson K, Stevens S, Jorgensen N, et al. ROR a -Mediated Purkinje Cell Development Determines Disease Severity in Adult SCA1 Mice. Cell. 2006;127:697–708.

63. Wang X, Allen M, Li S, Quicksall ZS, Patel TA, Carnwath TP, et al. Deciphering cellular transcriptional alterations in Alzheimer's disease brains. Mol. Neurodegener. Molecular Neurodegeneration; 2020;15:1–15.

64. Wieczorek L, Majumdar D, Wills TA, Hu L, Winder DG, Webb DJ, et al. Absence of Ca 2+-stimulated adenylyl cyclases leads to reduced synaptic plasticity and impaired experience-dependent fear memory. Transl. Psychiatry. 2012;2.

65. Ng SY, Bogu GK, Soh BS, Stanton LW. The long noncoding RNA RMST interacts with SOX2 to

regulate neurogenesis. Mol. Cell [Internet]. Elsevier Inc.; 2013;51:349–59. Available from: http://dx.doi.org/10.1016/j.molcel.2013.07.017

66. Cerrato V, Mercurio S, Leto K, Fucà E, Hoxha E, Bottes S, et al. Sox2 conditional mutation in mouse causes ataxic symptoms, cerebellar vermis hypoplasia, and postnatal defects of Bergmann glia. Glia. 2018;66:1929–46.

67. Kaur G, Levy E. Cystatin C in Alzheimer's disease. Front. Mol. Neurosci. 2012;5:1–11.

68. Zou J, Chen Z, Wei X, Chen Z, Fu Y, Yang X, et al. Cystatin C as a potential therapeutic mediator against Parkinson's disease via VEGF-induced angiogenesis and enhanced neuronal autophagy in neurovascular units. Cell Death Dis. [Internet]. Nature Publishing Group; 2017;8:e2854. Available from: http://dx.doi.org/10.1038/cddis.2017.240

69. Nagelhus EA, Ottersen OP. Physiological roles of Aquaporin-4 in brain. Physiol. Rev. 2013;93:1543–62.

70. Cvetanovic M. Decreased Expression of Glutamate Transporter GLAST in Bergmann Glia Is Associated with the Loss of Purkinje Neurons in the Spinocerebellar Ataxia Type 1. Cerebellum. 2015;14:8–11.

71. Li H, Xie Y, Zhang N, Yu Y, Zhang Q, Ding S. Disruption of IP3R2-mediated Ca2+ signaling pathway in astrocytes ameliorates neuronal death and brain damage while reducing behavioral deficits after focal ischemic stroke. Cell Calcium [Internet]. Elsevier Ltd; 2015;58:565–76. Available from: http://dx.doi.org/10.1016/j.ceca.2015.09.004

72. Farmer WT, Chierzi S, Lui C, Zaelzer C, Jones E V, Bally BP, et al. Neurons diversify astrocytes in the adult brain through sonic hedgehog signaling. Science (80-.). 2016;351:849.

73. Adolphe C, Nieuwenhuis E, Villani R, Li ZJ, Kaur P, Hui CC, et al. Patched 1 and patched 2 redundancy has a key role in regulating epidermal differentiation. J. Invest. Dermatol. [Internet]. Elsevier Masson SAS; 2014;134:1981–90. Available from: http://dx.doi.org/10.1038/jid.2014.63

74. DelRosso LM, Hoque R. The cerebellum and sleep. Neurol. Clin. [Internet]. Elsevier Inc; 2014;32:893–900. Available from: http://dx.doi.org/10.1016/j.ncl.2014.07.003

75. Pedroso JL, Braga-Neto P, Felício AC, Aquino CCH, do Prado LFB, do Prado GF, et al. Sleep disorders in cerebellar ataxias. Arq. Neuropsiquiatr. 2011;69:253–7.

76. Herculano-Houzel S. The glia/neuron ratio: How it varies uniformly across brain structures and species and what that means for brain physiology and evolution. Glia. 2014;62:1377–91.

77. O'Leary LA, Davoli MA, Belliveau C, Tanti A, Ma JC, Farmer WT, et al. Characterization of Vimentin-Immunoreactive Astrocytes in the Human Brain. Front. Neuroanat. 2020;14.

78. Janeczko K. CO-EXPRESSION OF GFAP AND VIMENTIN IN ASTROCYTES PROLIFERATING IN RESPONSE TO INJURY IN THE MOUSE CEREBRAL HEMISPHERE. A COMBINED AUTORADIOGRAPHIC AND DOUBLE IMMUNOCYTOCHEMICAL STUDY. Int J. Devl Neurocience. 1993;11:139–47.

79. Sen A, Nelson TJ, Alkon DL. ApoE isoforms differentially regulates cleavage and secretion of BDNF. Mol. Brain. Molecular Brain; 2017;10:1–7.

80. Ophir G, Meilin S, Efrati M, Chapman J, Karussis D, Roses A, et al. Human apoE3 but not apoE4 rescues impaired astrocyte activation in apoE null mice. Neurobiol. Dis. 2003;12:56–64.

81. Sharma M, Khan S, Rahman S, Singh LR. The extracellular protein, transthyretin is an oxidative stress biomarker. Front. Physiol. 2019;10:1–8.

82. Li X, Masliah E, Reixach N, Buxbaum JN. Neuronal production of transthyretin in human and murine alzheimer's disease: Is it protective? J. Neurosci. 2011;31:12483–90.

83. Parcerisas A, Ortega-Gascó A, Pujadas L, Soriano E. The hidden side of ncam family: Ncam2, a key cytoskeleton organization molecule regulating multiple neural functions. Int. J. Mol. Sci. 2021;22.

84. Baum ML, Wilton DK, Muthukumar A, Fox RG, Carey A, Crotty W, et al. CUB and Sushi Multiple Domains 1 (CSMD1) opposes the complement cascade in neural tissues. bioRxiv [Internet]. 2020;1:2020.09.11.291427. Available from: https://doi.org/10.1101/2020.09.11.291427

85. Cvetanovic M, Patel JM, Marti HH, Kini AR, Opal P. Vascular endothelial growth factor ameliorates the ataxic phenotype in a mouse model of spinocerebellar ataxia type 1. Nat Med [Internet]. 2011;17:1445–7. Available from:

http://www.ncbi.nlm.nih.gov/entrez/query.fcgi?cmd=Retrieve&db=PubMed&dopt=Citation&list_uids=22001907

86. Bradl M, Lassmann H. Oligodendrocytes: Biology and pathology. Acta Neuropathol. 2010;119:37–53.

87. Xin W, Mironova YA, Shen H, Marino RAM, Waisman A, Lamers WH, et al. Oligodendrocytes Support Neuronal Glutamatergic Transmission via Expression of Glutamine Synthetase. Cell Rep. [Internet]. ElsevierCompany.; 2019;27:2262-2271.e5. Available from: https://doi.org/10.1016/j.celrep.2019.04.094

88. Ben Haim L, Schirmer L, Zulji A, Sabeur K, Tiret B, Ribon M, et al. Evidence for glutamine synthetase function in mouse spinal cord oligodendrocytes. Glia. 2021;69:2812–27.

89. Ousman SS, Tomooka BH, Van Noort JM, Wawrousek EF, O'Conner K, Hafler DA, et al. Protective and therapeutic role for αB-crystallin in autoimmune demyelination. Nature. 2007;448:474–9.

90. Kuipers HF, Yoon J, Van Horssen J, Han MH, Bollyky PL, Palmer TD, et al. Phosphorylation of αB-crystallin supports reactive astrogliosis in demyelination. Proc. Natl. Acad. Sci. U. S. A. 2017;114:E1745–54.

91. Liu Y, Zhou Q, Tang M, Fu N, Shao W, Zhang S, et al. Upregulation of alphaB-crystallin expression in the substantia nigra of patients with Parkinson's disease. Neurobiol. Aging [Internet]. Elsevier Inc; 2015;36:1686–91. Available from: http://dx.doi.org/10.1016/j.neurobiolaging.2015.01.015

92. D'Agostino M, Scerra G, Cannata Serio M, Caporaso MG, Bonatti S, Renna M. Unconventional secretion of α-Crystallin B requires the Autophagic pathway and is controlled by phosphorylation of its serine 59 residue. Sci. Rep. 2019;9:1–14.

93. Behmoaras J, Bhangal G, Smith J, McDonald K, Mutch B, Lai PC, et al. Jund is a determinant of macrophage activation and is associated with glomerulonephritis susceptibility. Nat. Genet. 2008;40:553–9.

94. Rousseaux MWC, Tschumperlin T, Lu HC, Lackey EP, Bondar V V., Wan YW, et al. ATXN1-CIC

Complex Is the Primary Driver of Cerebellar Pathology in Spinocerebellar Ataxia Type 1 through a Gain-of-Function Mechanism. Neuron. 2018;97:1235-1243.e5.

95. Bell JJL, Lordkipanidze T, Cobb N. Bergmann glial ensheathment of dendritic spines regulates synapse number without affecting spine motility. Neuron Glia Biol. 2010;6:193–200.

96. Dell'Orco JM, Wasserman AH, Chopra R, Ingram MAC, Hu Y-S, Singh V, et al. Neuronal Atrophy Early in Degenerative Ataxia Is a Compensatory Mechanism to Regulate Membrane Excitability. J. Neurosci. [Internet]. 2015;35:11292–307. Available from: http://www.ncbi.nlm.nih.gov/pubmed/26269637%5Cnhttp://www.pubmedcentral.nih.gov/articlerender.fcgi?artid=PMC4532759

97. Nicita F, Tasca G, Nardella M, Bellacchio E, Camponeschi I, Vasco G, et al. Novel Homozygous KCNJ10 Mutation in a Patient with Non-syndromic Early-Onset Cerebellar Ataxia. The cerebellum. The Cerebellum; 2018;

98. Mellesmoen A, Sheeler C, Ferro A, Rainwater O, Cvetanovic M. Brain Derived Neurotrophic Factor (BDNF) Delays Onset of Pathogenesis in Transgenic Mouse Model of Spinocerebellar Ataxia Type 1 (SCA1). Front. Cell. Neurosci. 2019;12:1–8.

99. Sheeler C, Rosa J, Borgenheimer E, Mellesmoen A, Rainwater O. Post-symptomatic Delivery of Brain-Derived Neurotrophic Factor (BDNF) Ameliorates Spinocerebellar Ataxia Type 1 (SCA1) Pathogenesis. The Cerebellum. The Cerebellum; 2021;1.

100. Alshehri B, Pagnin M, Lee JY, Petratos S, Richardson SJ. The Role of Transthyretin in Oligodendrocyte Development. Sci. Rep. 2020;10:1–19.

101. Zhou L, Tang X, Li X, Bai Y, Buxbaum JN, Chen G. Identification of transthyretin as a novel interacting partner for the δ subunit of GABA A receptors. PLoS One. 2019;14:12–4.

102. Zawişlak A, Jakimowicz P, McCubrey JA, Rakus D. Neuron-derived transthyretin modulates astrocytic glycolysis in hormone-independent manner. Oncotarget. 2017;8:106625–38.

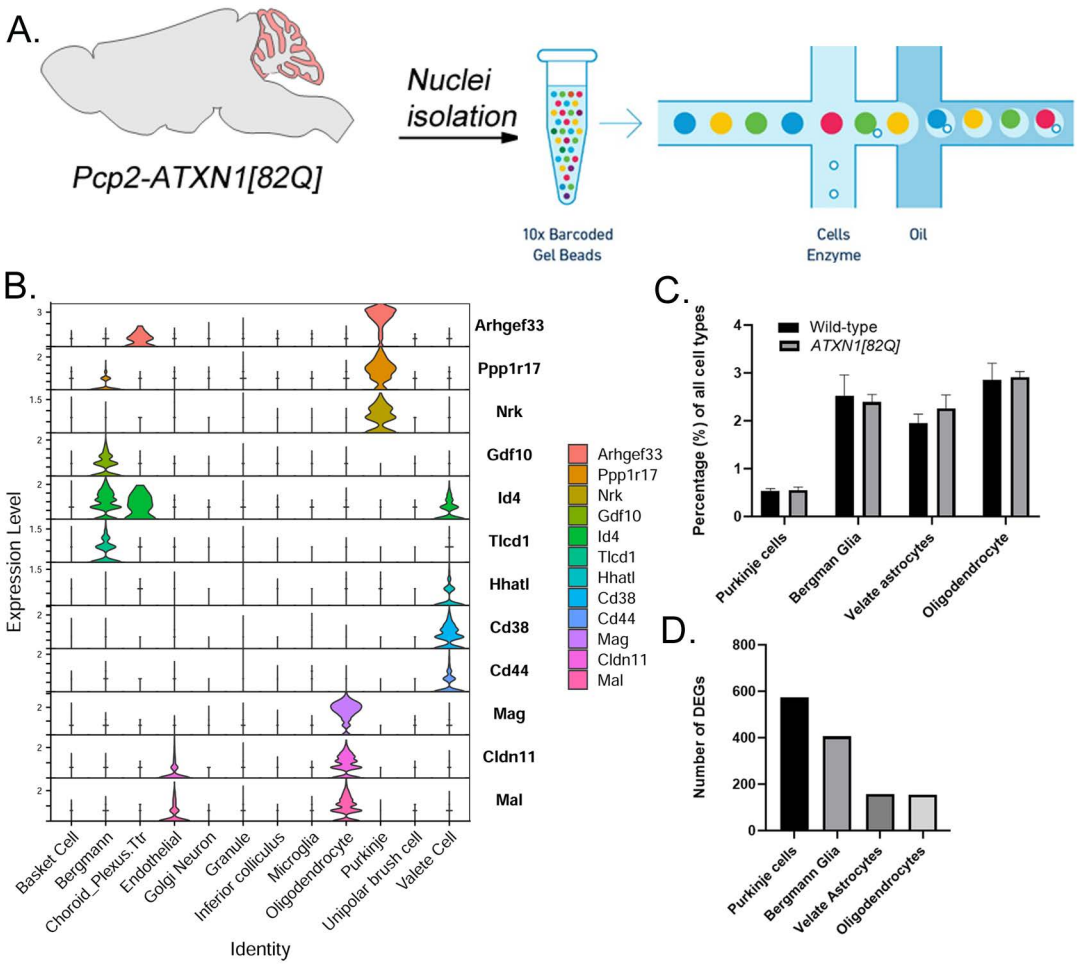
A.
Pcp2-ATXN1[82Q]
Nuclei isolation
10x Barcoded Gel Beads
Cells Enzyme
Oil
B.
Arhgef33
Ppp1r17
Nrk
Gdf10
Id4
Tlcd1
Hhatl
Cd38
Cd44
Mag
Cldn11
Mal
Expression Level
Basket Cell
Bergmann
Choroid_Plexus.Ttr
Endothelial
Golgi Neuron
Granule
Inferior colliculus
Microglia
Oligodendrocyte
Purkinje
Unipolar brush cell
Valete Cell
Identity
C.
Wild-type
ATXN1[82Q]
Percentage (%) of all cell types
Purkinje cells
Bergman Glia
Velate astrocytes
Oligodendrocyte
D.
Number of DEGs
Purkinje cells
Bergmann Glia
Velate Astrocytes
Oligodendrocytes

Figure 1.

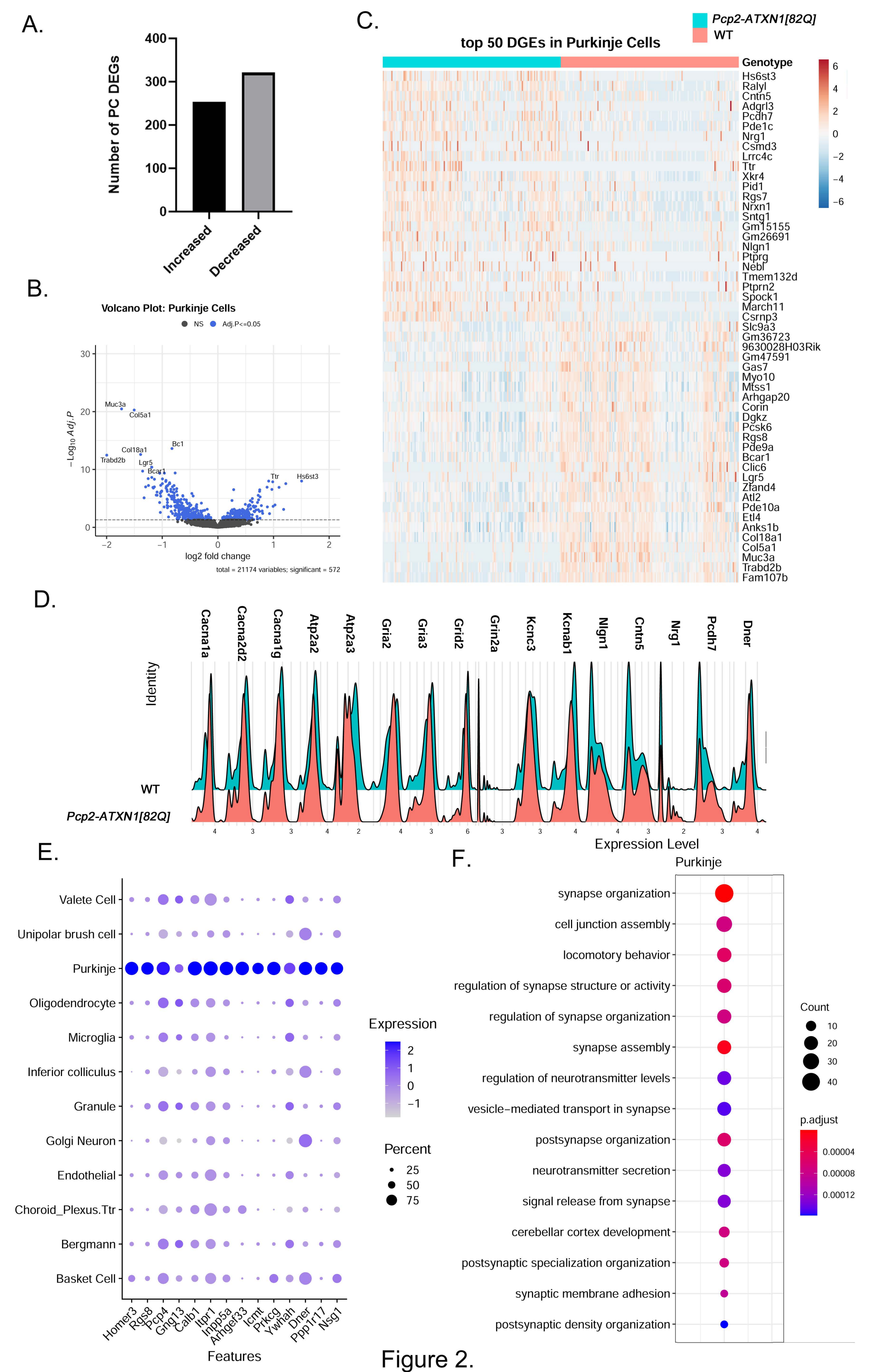
A.
Number of PC DEGs
400
300
200
100
0
Increased
Decreased
B.
Volcano Plot: Purkinje Cells
NS
Adj.P<=0.05
−Log10 Adj.P
Muc3a
Col5a1
Bc1
Col18a1
Trabd2b
Lgr5
Bcar1
Ttr
Hs6st3
log2 fold change
total = 21174 variables; significant = 572
C.
Pcp2-ATXN1[82Q]
WT
top 50 DGEs in Purkinje Cells
Genotype
Hs6st3
Ralyl
Cntn5
Adgrl3
Pcdh7
Pde1c
Nrg1
Csmd3
Lrrc4c
Ttr
Xkr4
Pid1
Rgs7
Nrxn1
Sntg1
Gm15155
Gm26691
Nlgn1
Ptprg
Nebl
Tmem132d
Ptprn2
Spock1
March11
Csrnp3
Slc9a3
Gm36723
9630028H03Rik
Gm47591
Gas7
Myo10
Mtss1
Arhgap20
Corin
Dgkz
Pcsk6
Rgs8
Pde9a
Bcar1
Clic6
Lgr5
Zfand4
Atl2
Pde10a
Etl4
Anks1b
Col18a1
Col5a1
Muc3a
Trabd2b
Fam107b
6
4
2
0
−2
−4
−6
D.
Cacna1a
Cacna2d2
Cacna1g
Atp2a2
Atp2a3
Gria2
Gria3
Grid2
Grin2a
Kcnc3
Kcnab1
Nlgn1
Cntn5
Nrg1
Pcdh7
Dner
Identity
WT
Pcp2-ATXN1[82Q]
Expression Level
E.
Valete Cell
Unipolar brush cell
Purkinje
Oligodendrocyte
Microglia
Inferior colliculus
Granule
Golgi Neuron
Endothelial
Choroid_Plexus.Ttr
Bergmann
Basket Cell
Homer3
Rgs8
Pcp4
Gng13
Calb1
Itpr1
Inpp5a
Arhgef33
Icmt
Prkcg
Ywhah
Dner
Ppp1r17
Nsg1
Features
Expression
2
1
0
−1
Percent
25
50
75
F.
Purkinje
synapse organization
cell junction assembly
locomotory behavior
regulation of synapse structure or activity
regulation of synapse organization
synapse assembly
regulation of neurotransmitter levels
vesicle−mediated transport in synapse
postsynapse organization
neurotransmitter secretion
signal release from synapse
cerebellar cortex development
postsynaptic specialization organization
synaptic membrane adhesion
postsynaptic density organization
Count
10
20
30
40
p.adjust
0.00004
0.00008
0.00012

Figure 2.

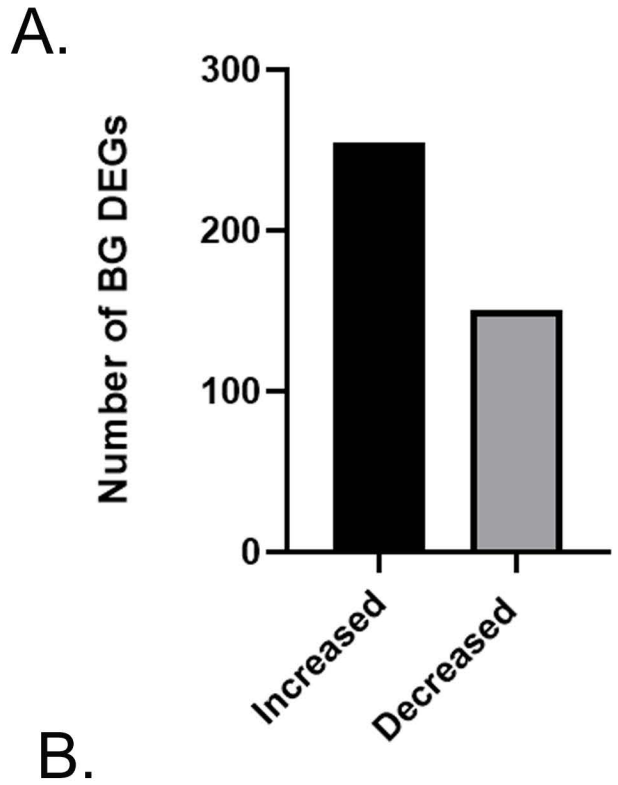
A.
Number of BG DEGs
300
200
100
0
Increased
Decreased

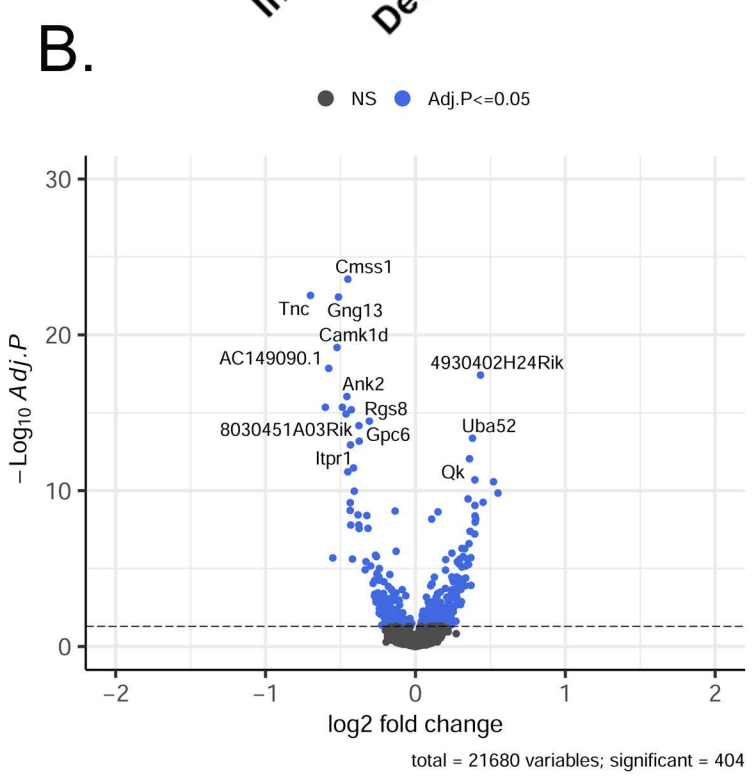
B.
NS
Adj.P<=0.05
−Log10 Adj.P
log2 fold change
Cmss1
Tnc
Gng13
Camk1d
AC149090.1
4930402H24Rik
Ank2
Rgs8
8030451A03Rik
Gpc6
Uba52
Itpr1
Qk
total = 21680 variables; significant = 404

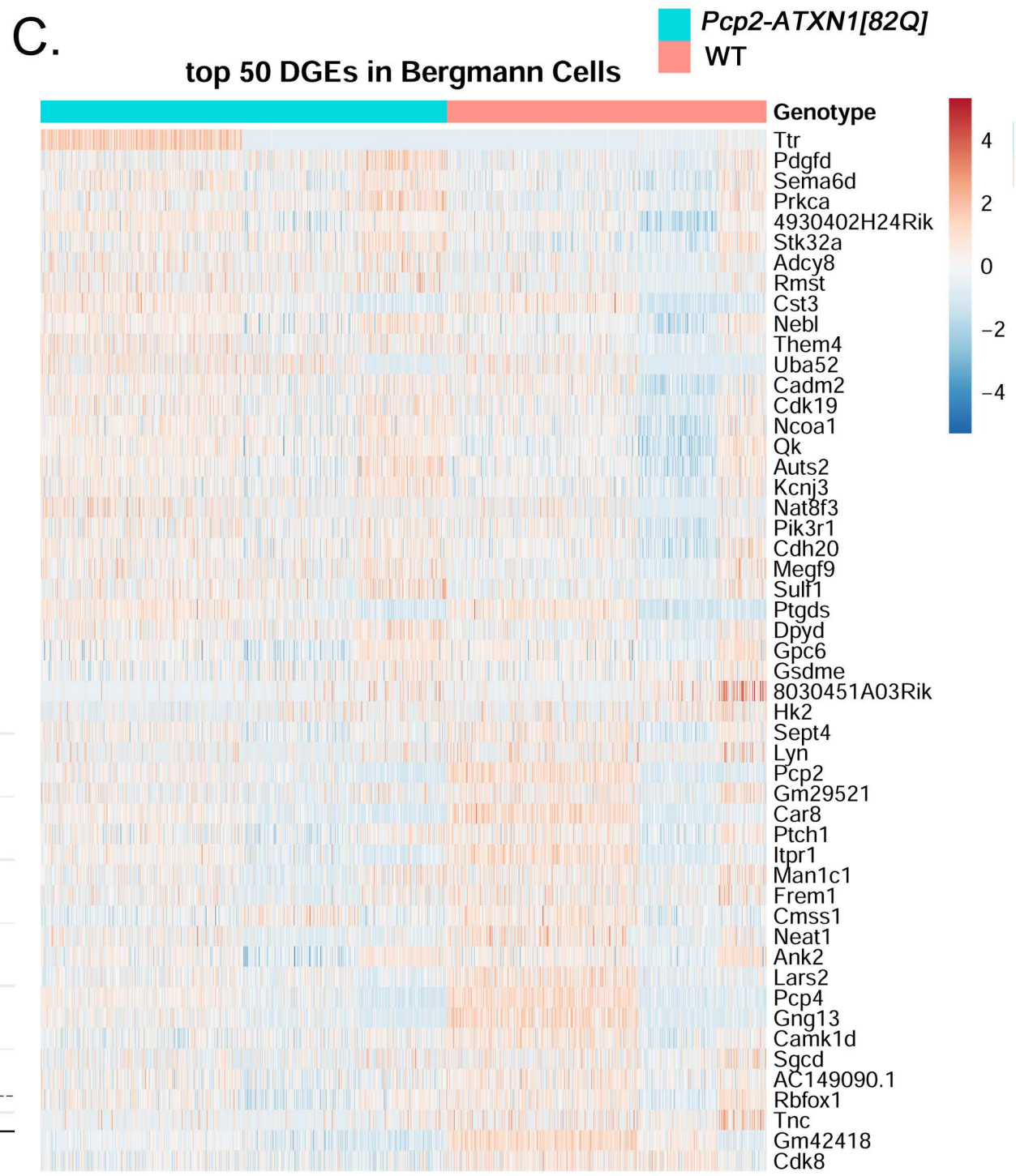
C.
Pcp2-ATXN1[82Q]
WT
top 50 DGEs in Bergmann Cells
Genotype
Ttr
Pdgfd
Sema6d
Prkca
4930402H24Rik
Stk32a
Adcy8
Rmst
Cst3
Nebl
Them4
Uba52
Cadm2
Cdk19
Ncoa1
Qk
Auts2
Kcnj3
Nat8f3
Pik3r1
Cdh20
Megf9
Sulf1
Ptgds
Dpyd
Gpc6
Gsdme
8030451A03Rik
Hk2
Sept4
Lyn
Pcp2
Gm29521
Car8
Ptch1
Itpr1
Man1c1
Frem1
Cmss1
Neat1
Ank2
Lars2
Pcp4
Gng13
Camk1d
Sgcd
AC149090.1
Rbfox1
Tnc
Gm42418
Cdk8

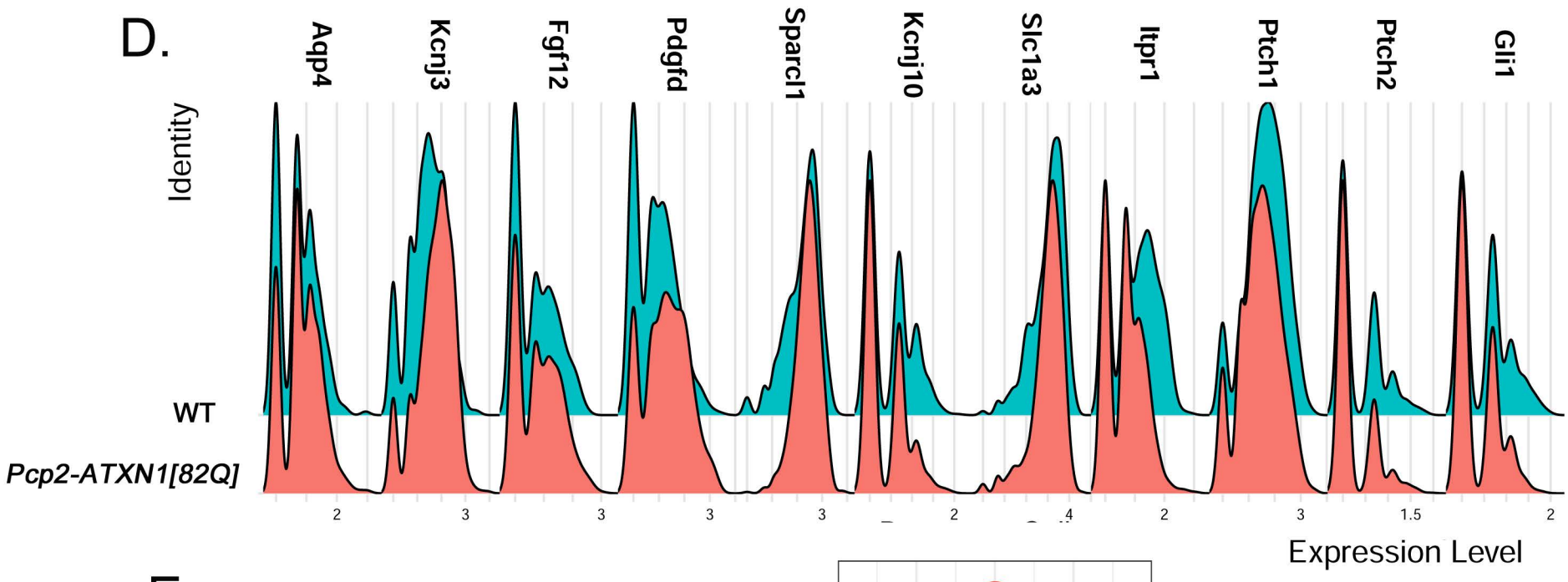
D.
Aqp4
Kcnj3
Fgf12
Pdgfd
Sparcl1
Kcnj10
Slc1a3
Itpr1
Ptch1
Ptch2
Gli1
Identity
WT
Pcp2-ATXN1[82Q]
Expression Level

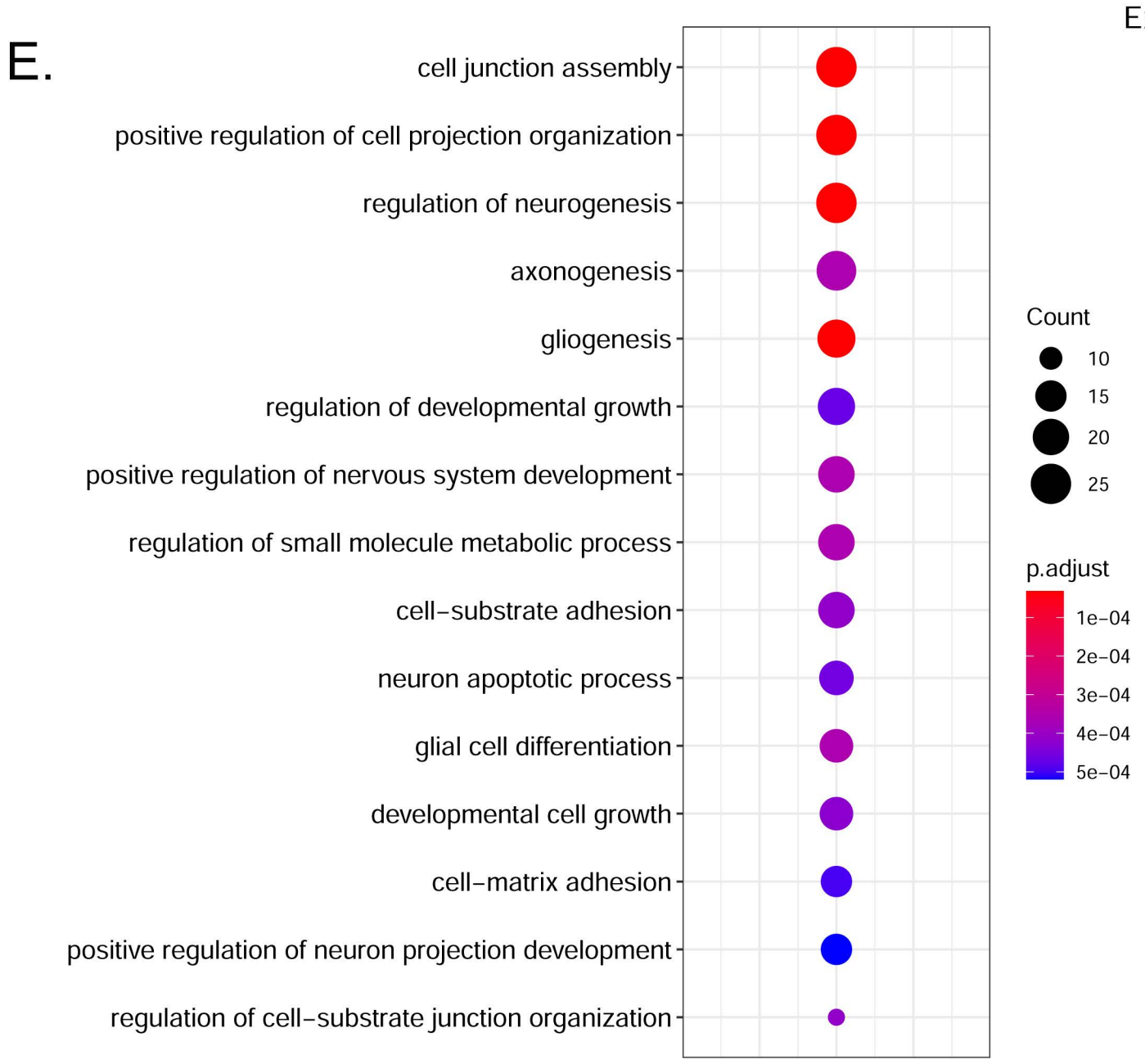
E.
cell junction assembly
positive regulation of cell projection organization
regulation of neurogenesis
axonogenesis
gliogenesis
regulation of developmental growth
positive regulation of nervous system development
regulation of small molecule metabolic process
cell−substrate adhesion
neuron apoptotic process
glial cell differentiation
developmental cell growth
cell−matrix adhesion
positive regulation of neuron projection development
regulation of cell−substrate junction organization
Count
10
15
20
25
p.adjust
1e−04
2e−04
3e−04
4e−04
5e−04

Figure 3.

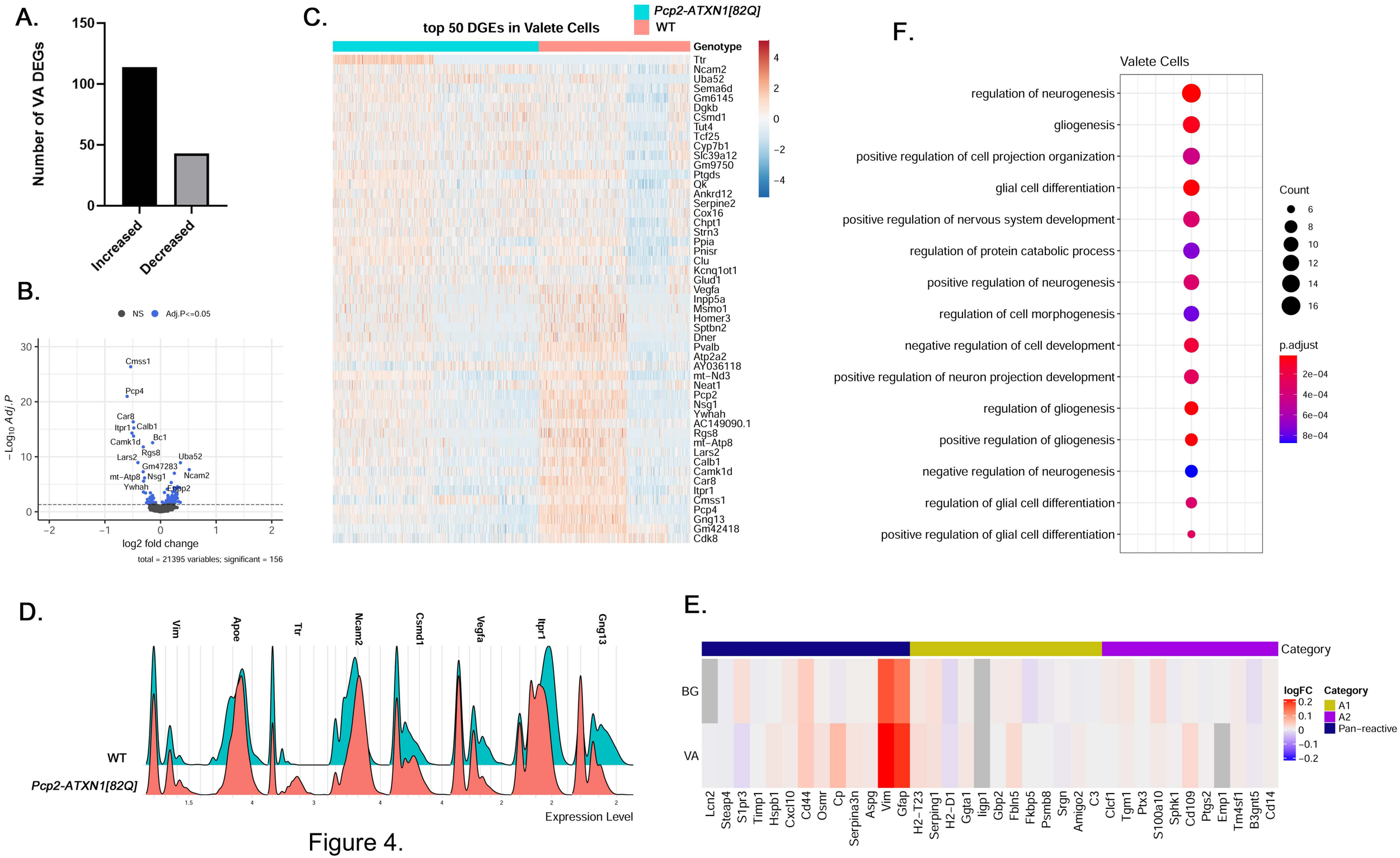
A.
Number of VA DEGs
150
100
50
0
Increased
Decreased
B.
NS
Adj.P<=0.05
−Log10 Adj.P
log2 fold change
Cmss1
Pcp4
Car8
Itpr1
Calb1
Camk1d
Bc1
Rgs8
Lars2
Uba52
Gm47283
mt−Atp8
Nsg1
Ncam2
Ywhah
Enpp2
total = 21395 variables; significant = 156
C.
top 50 DGEs in Valete Cells
Pcp2-ATXN1[82Q]
WT
Genotype
Ttr
Ncam2
Uba52
Sema6d
Gm6145
Dgkb
Csmd1
Tut4
Tcf25
Cyp7b1
Slc39a12
Gm9750
Ptgds
Qk
Ankrd12
Serpine2
Cox16
Chpt1
Strn3
Ppia
Pnisr
Clu
Kcnq1ot1
Glud1
Vegfa
Inpp5a
Msmo1
Homer3
Sptbn2
Dner
Pvalb
Atp2a2
AY036118
mt−Nd3
Neat1
Pcp2
Nsg1
Ywhah
AC149090.1
Rgs8
mt−Atp8
Lars2
Calb1
Camk1d
Car8
Itpr1
Cmss1
Pcp4
Gng13
Gm42418
Cdk8
F.
Valete Cells
regulation of neurogenesis
gliogenesis
positive regulation of cell projection organization
glial cell differentiation
positive regulation of nervous system development
regulation of protein catabolic process
positive regulation of neurogenesis
regulation of cell morphogenesis
negative regulation of cell development
positive regulation of neuron projection development
regulation of gliogenesis
positive regulation of gliogenesis
negative regulation of neurogenesis
regulation of glial cell differentiation
positive regulation of glial cell differentiation
Count
p.adjust
D.
Vim
Apoe
Ttr
Ncam2
Csmd1
Vegfa
Itpr1
Gng13
WT
Pcp2-ATXN1[82Q]
Expression Level
E.
Category
BG
VA
logFC
Category
A1
A2
Pan−reactive
Lcn2
Steap4
S1pr3
Timp1
Hspb1
Cxcl10
Cd44
Osmr
Cp
Serpina3n
Aspg
Vim
Gfap
H2−T23
Serping1
H2−D1
Ggta1
Iigp1
Gbp2
Fbln5
Fkbp5
Psmb8
Srgn
Amigo2
C3
Clcf1
Tgm1
Ptx3
S100a10
Sphk1
Cd109
Ptgs2
Emp1
Tm4sf1
B3gnt5
Cd14

Figure 4.

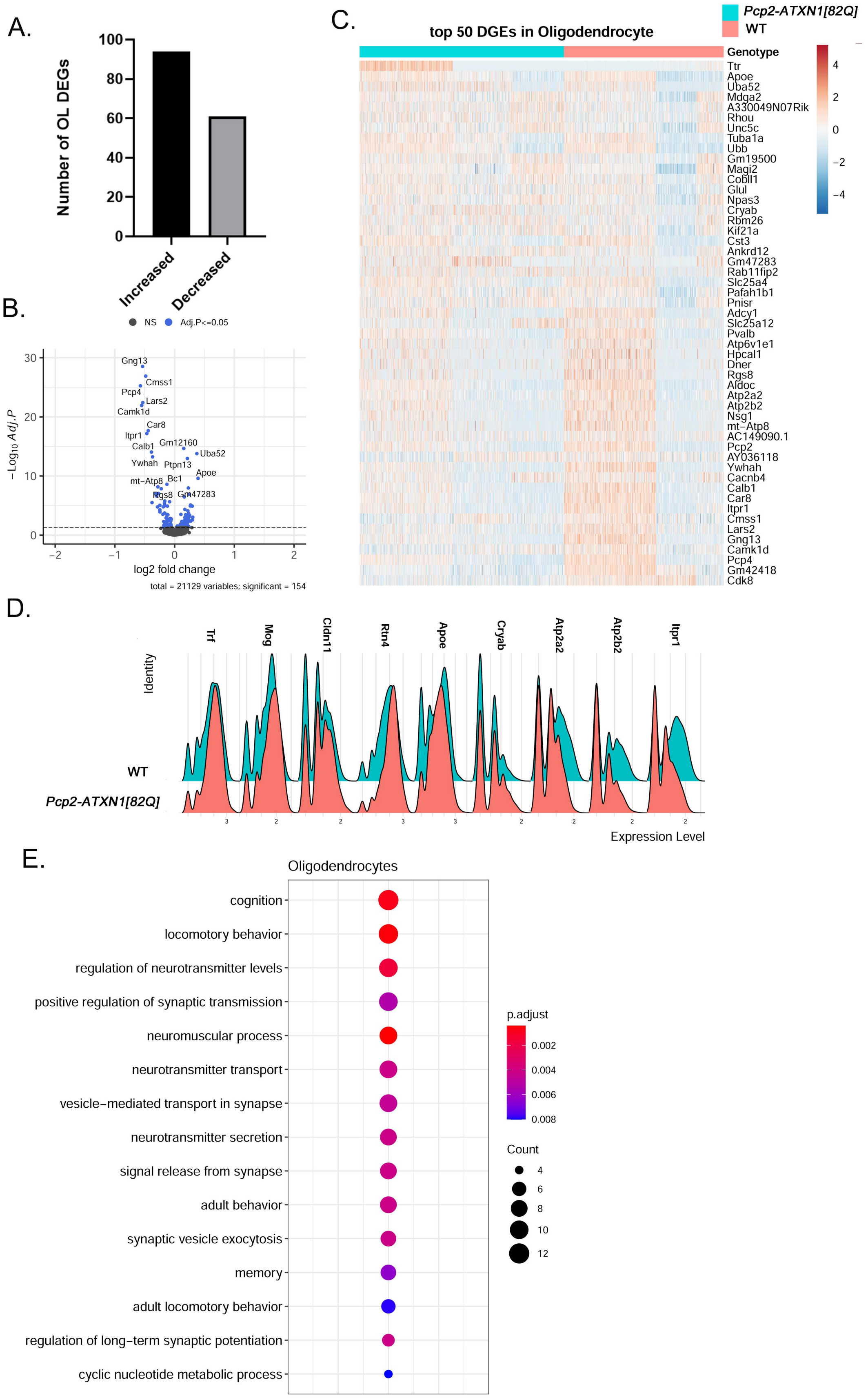
A.
Number of OL DEGs
100
80
60
40
20
0
Increased
Decreased
NS
Adj.P<=0.05
B.
−Log10 Adj.P
log2 fold change
Gng13
Cmss1
Pcp4
Lars2
Camk1d
Car8
Itpr1
Calb1
Gm12160
Uba52
Ywhah
Ptpn13
Apoe
mt−Atp8
Bc1
Rgs8
Gm47283
total = 21129 variables; significant = 154
C.
top 50 DGEs in Oligodendrocyte
Pcp2-ATXN1[82Q]
WT
Genotype
Ttr
Apoe
Uba52
Mdga2
A330049N07Rik
Rhou
Unc5c
Tuba1a
Ubb
Gm19500
Magi2
Cobll1
Glul
Npas3
Cryab
Rbm26
Kif21a
Cst3
Ankrd12
Gm47283
Rab11fip2
Slc25a4
Pafah1b1
Pnisr
Adcy1
Slc25a12
Pvalb
Atp6v1e1
Hpcal1
Dner
Rgs8
Aldoc
Atp2a2
Atp2b2
Nsg1
mt−Atp8
AC149090.1
Pcp2
AY036118
Ywhah
Cacnb4
Calb1
Car8
Itpr1
Cmss1
Lars2
Gng13
Camk1d
Pcp4
Gm42418
Cdk8
D.
Trf
Mog
Cldn11
Rtn4
Apoe
Cryab
Atp2a2
Atp2b2
Itpr1
Identity
WT
Pcp2-ATXN1[82Q]
Expression Level
E.
Oligodendrocytes
cognition
locomotory behavior
regulation of neurotransmitter levels
positive regulation of synaptic transmission
neuromuscular process
neurotransmitter transport
vesicle−mediated transport in synapse
neurotransmitter secretion
signal release from synapse
adult behavior
synaptic vesicle exocytosis
memory
adult locomotory behavior
regulation of long−term synaptic potentiation
cyclic nucleotide metabolic process
p.adjust
0.002
0.004
0.006
0.008
Count
4
6
8
10
12

Figure 5.